

UCLA

UCLA Electronic Theses and Dissertations

Title

Multi Negative Feedback Loops and Nonlinear Time-Delays in a Mathematical Model of Bone Morphogenetic Protein (BMP) Signaling in Vascular Endothelial Cells

Permalink

<https://escholarship.org/uc/item/5m96170m>

Author

Nia, Anna Mohtasham

Publication Date

2015

Peer reviewed|Thesis/dissertation

UNIVERSITY OF CALIFORNIA
Los Angeles

Multi Negative Feedback Loops and Nonlinear Time-Delays in a Mathematical Model of
Bone Morphogenetic Protein (BMP) Signaling in Vascular Endothelial Cells

A thesis submitted in partial satisfaction
of the requirements for the degree
Master of Science in Bioengineering

by

Anna Mohtasham Nia

2015

© Copyright by
Anna Mohtasham Nia
2015

ABSTRACT OF THE THESIS

Multi Negative Feedback Loops and Nonlinear Time-Delays in a Mathematical Model of
Bone Morphogenetic Protein (BMP) Signaling in Vascular Endothelial Cells

by

Anna Mohtasham Nia

Master of Science in Bioengineering

University of California, Los Angeles, 2015

Professor Alan Garfinkel, Chair

Negative feedback loops are well known in physiology. Previous work at UCLA has identified a negative feedback pathway involving Bone Morphogenetic Protein 4 (BMP-4) and an inhibitor of BMP-4 called Matrix Gla Protein (MGP) active in vascular development and pathology.[28] More recently, other inhibitors of BMP-4 have been identified in vascular tissue, including Crossveinless 2 (CV-2). In addition, experimental works performed by our collaborators at Dr. Bostrom's lab have identified oscillations in the concentrations of these morphogens gene expressions.

We developed a mathematical model of the interactions among the new, larger set of morphogens. In particular, there are at least 2 negative feedback loops, one acting with a short time delay and the other acting with a longer time delay. In fact, there are 3 distinct time delays in our mathematical model. The goal was to understand what conditions would give rise to sustained oscillations in this model. With a view to comparing these results to experimental observations in the lab of Dr. Kristina Bostrom at UCLA, we have attempted to draw general conclusions about the behavior of multiple loop feedback systems, a problem of general interest.

The thesis of Anna Mohtasham Nia is approved.

Zhilin Qu

Daniel Ennis

Alan Garfinkel, Committee Chair

University of California, Los Angeles

2015

*To my mother and father, Parvin and Arsalan Nia . . .
whose words of encouragement and push for tenacity ring in my ears.
My brother Ardavon, who among so many other things—
never left my side and always supported me to pursue my aspirations.
I also dedicate this thesis to my best friend Rommina Ghavami,
for being a sister I always wished for . . .
and for always being there for me throughout the entire graduate program at UCLA.*

TABLE OF CONTENTS

1	Introduction	1
1.1	Oscillating Systems	1
1.2	Nonlinear Oscillators and Complex Dynamical Behavior	2
1.3	Time Delays in Biological Oscillations	3
1.4	Feedback Control and Cellular Differentiation	5
1.5	The BMP Regulatory Network	8
1.6	Simplified BMP Network Diagram of the Mathematical Model	9
1.7	Motivation	12
2	Methods	14
2.1	The Non-Linear Time Delay Mathematical Model	14
2.2	BMP ODE System	17
2.3	Parameter Estimation	18
2.3.1	Production Rates	19
2.3.2	Degradation Rates	19
2.3.3	Time Delays and Coefficients	20
2.4	Stability, Equilibrium Points and Steady State Analysis	21
2.4.1	Numerical Integration Algorithm	21
2.4.2	State Space Geometry	21
2.4.3	Equilibrium	23
2.5	Oscillation Period Analysis with the Fourier Transform Method	24
3	Results	25
3.1	System Simulations Using Parameter Estimation Table 2.1	25

3.2	System's Equilibria and Stability	25
3.3	Oscillation Simulation of the Model	26
3.4	Fourier Analysis Results	26
4	Discussion	53
4.1	Time Delay Analysis using the Fourier Transform Method	56
4.2	Conclusion	56
	References	58

LIST OF FIGURES

1.1	Compartment Diagram of the HPA Axis [3]	5
1.2	Cortisol Data in Patients [3]	6
1.3	ALK-1 mRNA Expression	7
1.4	A pattern formation in cultured VMCs in vitro. Over 20 days, VMCs plated in vitro develop from a monolayer of randomly oriented cells of nearly uniform density (approximately day 1; stage 1) (a), to local alignment of cells into regions (swirls) of nearly uniform size (approximately day 4; stage 2) (b), to ridges of high cell density (dark areas) (approximately day 10; stage 3) (c), to connected ridges forming a labyrinthine pattern (approximately day 16; stage 4) (von Kossa stain) (d). (e) At 3 higher magnification, a phase-contrast image of an unstained ridge shows the perpendicular orientation of cells in the monolayer relative to the edges of the multicellular ridge. [Bar = 250 m(a and b); c and d are at the same magnification as b; bar in e shows the approximate size, shape, and orientation of a single cell ([28]).	10
1.5	Numerical solutions of the mathematical model corresponding to each of the stages from figure 1.4 ([28]).	11
1.6	BMP Network Diagram: Network diagram for biological relationship accounted for in the model. BMP-9 endogenous ligands bind to ALK-1 receptor along with its co-receptor endoglin to stimulate production of CV-2 and MGP with a transcriptional time delay of τ_1 and τ_2 respectively. CV-2 and MGP bind and inhibit BMP-9 and BMP-4, respectively. BMP-4 autocatalytically produces itself and activates ALK-1 transcription with a time delay of τ_3 . BMP-4 signaling is associated with EC progenitor state and it is angiogenic, while BMP-9/ALK-1 signaling stimulates EC differentiation and it is anti-angiogenic.	13

3.1	Temporal responses for the mathematical model of BMP using the parameter values estimated 2.1 and all initial conditions were set to 1.	26
3.2	Temporal responses for the individual variables in the mathematical model of BMP using the parameter values estimated 2.1 and all initial conditions were set to 1.	27
3.3	State Space Diagram: state space solution are illustrated in 3D plot for BMP-9, BMP-4 and Endoglin shown in 3.2.	28
3.4	State Space Diagram: state space solutions are illustrated in 3D plot for MGP, CV-2 and ALK-1 shown in 3.2.	29
3.5	The simulation results of the model: Temporal responses for the mathematical model of BMP using the parameter values estimated 2.1, but using different degradation rates for BMP-9 at 65 percent, Endoglin, MGP, and CV-2 at 80 percent and ALK-1 at 15 percent of their production rates. . . .	30
3.6	The simulation results of the model: Temporal responses for the individual variables of BMP using the parameter values estimated 2.1, but using different degradation rates for BMP-9 at 65 percent, Endoglin, MGP, and CV-2 at 80 percent and ALK-1 at 15 percent of their production rates. . . .	31
3.7	State Space Diagram: state space solution are illustrated in 3D plot for BMP-9, BMP-4 and Endoglin shown in 3.6.	32
3.8	State Space Diagram: state space solutions are illustrated in 3D plot for MGP, CV-2 and ALK-1 shown in 3.6.	33
3.9	Fourier Analysis of BMP-9: Oscillation periods are shown with different time delays for MGP and CV-2 transcription while keeping ALK-1 transcriptional time delay constant at 8 hours. All parameters are used from 3.5. . . .	35
3.10	Fourier Analysis of BMP-9: Oscillation periods are shown with different time delays for MGP and ALK-1 transcription while keeping CV-2 transcriptional time delay constant at 11 hours. All parameters are used from 3.5. . . .	36

3.11	Fourier Analysis of BMP-9: Oscillation periods are shown with different time delays for CV-2 and ALK-1 transcription while keeping MGP transcriptional time delay constant at 4 hours. All parameters are used from 3.5. . . .	37
3.12	Fourier Analysis of BMP-4: Oscillation periods are shown with different time delays for MGP and CV-2 transcription while keeping ALK-1 transcriptional time delay constant at 8 hours. All parameters are used from 3.5. . . .	38
3.13	Fourier Analysis of BMP-4: Oscillation periods are shown with different time delays for MGP and ALK-1 transcription while keeping CV-2 transcriptional time delay constant at 11 hours. All parameters are used from 3.5. . . .	39
3.14	Fourier Analysis of BMP-4: Oscillation periods are shown with different time delays for CV-2 and ALK-1 transcription while keeping MGP transcriptional time delay constant at 4 hours. All parameters are used from 3.5. . . .	40
3.15	Fourier Analysis of Endoglin: Oscillation periods are shown with different time delays for MGP and CV-2 transcription while keeping ALK-1 transcriptional time delay constant at 8 hours. All parameters are used from 3.5. . . .	41
3.16	Fourier Analysis of Endoglin: Oscillation periods are shown with different time delays for MGP and ALK-1 transcription while keeping CV-2 transcriptional time delay constant at 11 hours. All parameters are used from 3.5. . . .	42
3.17	Fourier Analysis of Endoglin: Oscillation periods are shown with different time delays for CV-2 and ALK-1 transcription while keeping MGP transcriptional time delay constant at 4 hours. All parameters are used from 3.5. . . .	43
3.18	Fourier Analysis of MGP: Oscillation periods are shown with different time delays for MGP and CV-2 transcription while keeping ALK-1 transcriptional time delay constant at 8 hours. All parameters are used from 3.5.	44
3.19	Fourier Analysis of MGP: Oscillation periods are shown with different time delays for MGP and ALK-1 transcription while keeping CV-2 transcriptional time delay constant at 11 hours. All parameters are used from 3.5.	45

3.20	Fourier Analysis of MGP: Oscillation periods are shown with different time delays for CV-2 and ALK-1 transcription while keeping MGP transcriptional time delay constant at 4 hours. All parameters are used from 3.5	46
3.21	Fourier Analysis of CV-2: Oscillation periods are shown with different time delays for MGP and CV-2 transcription while keeping ALK-1 transcriptional time delay constant at 8 hours. All parameters are used from 3.5.	47
3.22	Fourier Analysis of CV-2: Oscillation periods are shown with different time delays for MGP and ALK-1 transcription while keeping CV-2 transcriptional time delay constant at 11 hours. All parameters are used from 3.5.	48
3.23	Fourier Analysis of CV-2: Oscillation periods are shown with different time delays for CV-2 and ALK-1 transcription while keeping MGP transcriptional time delay constant at 4 hours. All parameters are used from 3.5	49
3.24	Fourier Analysis of ALK-1: Oscillation periods are shown with different time delays for MGP and CV-2 transcription while keeping ALK-1 transcriptional time delay constant at 8 hours. All parameters are used from 3.5.	50
3.25	Fourier Analysis of ALK-1: Oscillation periods are shown with different time delays for MGP and ALK-1 transcription while keeping CV-2 transcriptional time delay constant at 11 hours. All parameters are used from 3.5.	51
3.26	Fourier Analysis of ALK-1: Oscillation periods are shown with different time delays for CV-2 and ALK-1 transcription while keeping MGP transcriptional time delay constant at 4 hours. All parameters are used from 3.5	52

LIST OF TABLES

2.1	Model Parameters: This table contains the approximate values, units and the biological functions of parameters used in this study.	22
-----	--	----

ACKNOWLEDGMENTS

First and foremost I want to thank my advisor, Dr. Alan Garfinkel for all his contributions of time, and ideas to make my graduate school experience productive and intellectually stimulating. I hope I could be as lively, enthusiastic, and motivated as Alan and to someday be able to command an audience as well as he can. I am thankful for the excellent example he has provided as a successful scientist and professor. He has taught me, how important mathematical models are in every aspect of our lives and I hope to carry the knowledge of nonlinear dynamics and chaos with me throughout my career as a physician scientist.

I am very grateful to a member of our lab, Dr. Yina Guo for her scientific advice, knowledge and many insightful discussions and suggestions. I would also like to thank our experimental collaborators Dr. Kristina Bostrom and Dr. Pierre Guihard for whom without, this project would have not been possible.

I would also like to acknowledge and thank my committee members Dr. Daniel Ennis and Dr. Zhilin Qu who were more than generous with their expertise and precious time.

CHAPTER 1

Introduction

1.1 Oscillating Systems

Oscillating systems are abundant in nature. To name just a few, your body temperature, the pendulum on your grandfather's clock, your sleep pattern cycle, and so on. We are all used to observing oscillations throughout our everyday lives, but understanding what it exactly takes to demonstrate these kind of oscillations is a daunting task. One way to generalize oscillating systems are damped and un-damped (sustained) oscillations. Another way to classify are through free or forced oscillations. In our study, we are more concerned with the distinction between damped and un-damped oscillation. In a damped oscillation, the amplitude of the oscillation will be reduced to zero as there will be no compensation for the the energy loss. However, in an un-damped oscillation the oscillation continues; therefore, they are called sustained oscillations or continuous waves.

Oscillations are essential property of every living systems. Currently, there are numerous examples of biological oscillators in the scientific literature. Many of them have addressed the mathematical basis of these general oscillatory phenomenon ([18],[34],[27],[31],[41]). Oscillations play a pivotal role in many dynamic cellular processes, and contribute to the patho-physiology of many diseases. As an example, a diverse collection of neuroendocrine responses and signals occur along the hypothalamic-pituitary-adrenal axis (HPA axis). The HPA axis is a prominent example of a dynamical biological system constantly at work. It is functionally related to other systems in the body. Perturbation to the system causing a sustained elevation of the cortisol level (hypercortisolism) has been reported in patients with depression, diabetes, obesity, and Cushing syndrome (CS)([21, 47, 42]). Also, diseases

that suppress the adrenal cortex lead to cortisol insufficiency (hypo-cortisolism) have been reported in patients with Addison's disease. A common feature among all these patients are oscillations at signature frequencies. The origin of these different oscillatory behaviors depend upon numerous factors from different biological systems at work simultaneously. This is just one example to represent the crucial effect of oscillatory dynamics in our physiology and health.

Many oscillatory systems share common features. Scientists would like to identify these mechanisms and feature in order to identify general principles that underlie the existence of dynamic behaviors in numerous biological systems. System biology addresses such questions by studying the the complex behaviors of these oscillating system through theoretical and experimental analysis ([34]).

1.2 Nonlinear Oscillators and Complex Dynamical Behavior

When we learn about oscillations, we often hear about linear oscillators and their properties. We all learned about the simple oscillator in our high school physics class. Our simple examples were mass on a spring or a cork floating in water. In our macroscopic world, no system is actually a simple oscillator. Dissipative forces are always present even though we are used to ignore them in order to simplify the problems. A linear oscillator only oscillates with one frequency; its motion is frequently characterized by a sinusoidal wave equation along with its period and angular frequency. If we have a restorative force that is not linear in the system, the oscillations will no longer have a single frequency even though the waves would still repeat themselves. That is a feature of a nonlinear oscillating system.

Non-linear oscillators are the building blocks of a complex motion. The motion of a non-linear oscillator consists of complex behavior that is made up of harmonics of its fundamental frequency. Whether you see one frequency more than the other depends upon the details of the non-linearity and interaction of the terms in the mathematical equations. A good example of a nonlinear oscillator is a pendulum. The pendulum is not a simple oscillator,

but it is rather a nonlinear one since its frequency decreases with increasing amplitude.

Over the years, the ideas and techniques of nonlinear dynamics and chaos have been used extensively in biology, even though it was originally a branch of physics where Newton invented differential equations in order to describe the laws of motion and universal gravitation in the mid-1600s. He developed extensive analytical methods to solve the two-body problem. When scientists tried to use his mathematical methods to solve the three-body problem, they realized it was essentially impossible to solve ([57]). In the late 1800s, Poincare made a breakthrough by introducing qualitative analysis rather than quantitative. His geometric insights into answering complex questions rendered the study of complex systems possible. In our study, we use nonlinear techniques to study bone morphogenetic protein (BMP) regulatory network. Specifically, the BMP-4/9 network in endothelial cells.

1.3 Time Delays in Biological Oscillations

Complex rhythms are ubiquitous in physiological systems. Mathematical biologists have been using ordinary and partial differential equations to model the dynamics of these physiological systems for decades. Lotka and Volterra, Verhulst, and Malthus, to name a few, have provided us with a better quantification of these complex biological phenomena, as all of these models have many assumptions built into them. It is obvious that no model can truly capture the complexity of the dynamics observed in real biological phenomena. Therefore, mathematical biologists always look for better approaches to model these complexities with fewer and better assumptions. We can raise the number of ordinary or partial differential equations to capture more complexity, but the downfall of that would be dealing with a large number of parameters that are often difficult if not impossible to pin down. Investigating which parameters are crucial to describe a biological process is a very challenging task and oftentimes it requires experimental work in order to estimate a physiologically meaningful range for a given parameter.

One approach that have been used to model the complex biological rhythms are the

usage of time delays in systems of differential equations. Current evidence suggests that time delays play an important role in a design of many of these biological feedback control systems. The presence of dual-delayed feedback mechanisms have been observed numerous times in many biological systems. One prominent example of time delays is demonstrated in the HPA axis model mentioned earlier in this chapter.

When modeling the HPA axis, circadian rhythm and ultradian rhythm were considered two different characteristics of this system, with circadian rhythm characterized as an external input of the system in a 24-hour cycle and ultradian rhythm as an inherent characteristic of the system. Regardless of these two general beliefs, a system of coupled non-linear ordinary differential equations with oscillating solution curves have always been modeled mainly because they have been in line with experimental data showing cortisol concentration in hypercortisolic, hypocortisolic, and normal individuals ([2]). The model presented by [63] consists of three coupled nonlinear ordinary differential equations called minimal model trying to exemplify the general case. Their minimal model has a locally stable fixed point using parameters that were obtained either from the literature, or using physiological reasoning. It is shown that a perturbation to any of these parameters led to global stability of the fixed point, and when using these parameters, no oscillating solutions were possible. Therefore, the aforementioned model could not account for the ultradian rhythm observed in cortisol experimental data when using the minimal model and physiologically meaningful parameter values. Anderson et al. 2013, later proposed that some important mechanisms were missing from the model such as hippocampal effects that could introduce important dynamical properties to the model or time delays which could present the possibility of ultradian rhythm and limit cycles. When time delays were used, the oscillatory regimes that were in line with clinical data could be observed. The use of time delays was explained by the time it takes for the hormones to travel in the bloodstream and to bind to receptors ([2]).

Much of the complexity observed in these control biological systems can be captured through time delay dynamics. Biological systems by nature have intrinsic delays, and math-

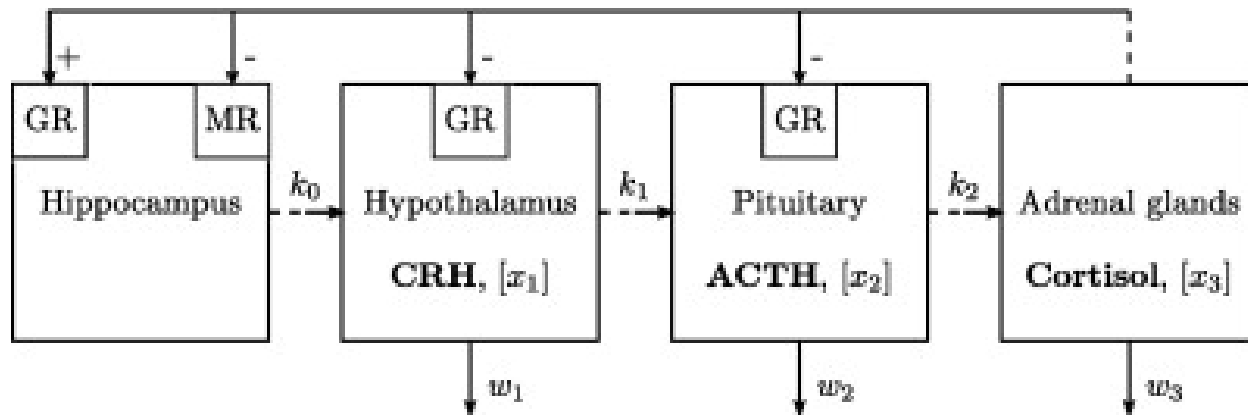


Figure 1.1: Compartment Diagram of the HPA Axis [3]

emantics of these time delayed systems are compelling and pose many analytical challenges. In this work, we try to investigate time delays in the BMP regulatory network and their effects on the system's dynamics.

1.4 Feedback Control and Cellular Differentiation

Feedback control systems have been long considered as a basis to ensure homeostasis. Gene networks are no exceptions and constantly use both positive and negative feedback regulatory control systems in order to regulate their own expression. As an example, positive feedback and autocatalysis have been identified in bistable responses in chemical reactions ([9]). In a bistable system, when one or more system's parameters are changed, the system can make a transition between stability and instability. In theoretical models, positive and negative feedback systems have been shown to produce a variety of dynamical behaviors ([25]). The HPA axis model described above was an example of a negative feedback model that produced many complex dynamics in patients.

Bone morphogenetic proteins (BMP) are a part of the TGF- β superfamily, which primarily induce bone formation. In mammals, there are at least 12 BMPs. BMPs have been conserved throughout evolution and have been shown to rescue a patterning defect in BMP-2/4 null *Drosophila* ([44]). As the name suggests, Bone morphogenetic proteins play

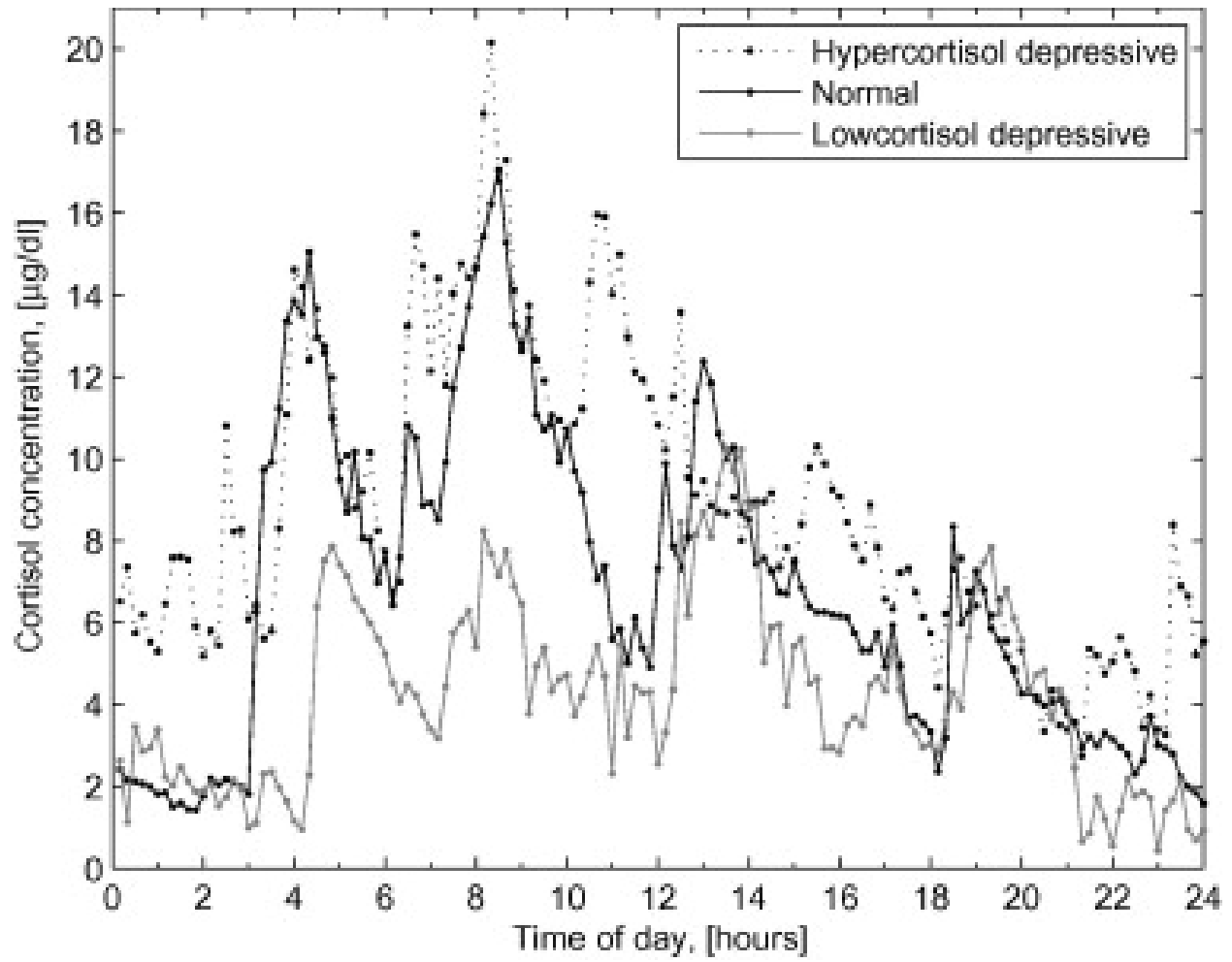


Figure 1.2: Cortisol Data in Patients [3]

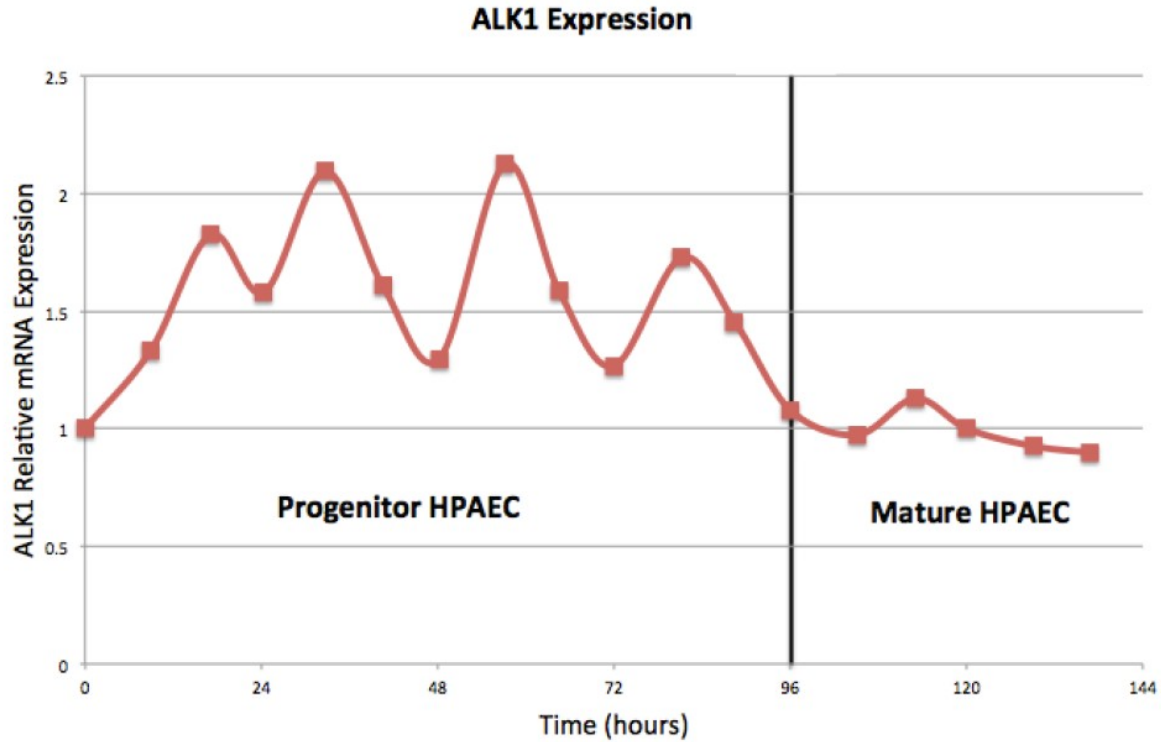


Figure 1.3: ALK-1 mRNA Expression

important roles in morphogenesis and cell differentiation. Oscillatory gene expression has been identified to maintain the progenitor status of the cell.

Our collaborators in Dr. Kristina Bostrom's Lab at UCLA have identified oscillatory gene expression patterns in several proteins in the BMP regulatory network in human pulmonary vascular endothelial cells (HPAECs) that transition to non-oscillatory regime upon cellular differentiation. Like the HPA axis, the BMP network also consists of negative feedback loops that makes its dynamical behavior interesting. The effect of negative feedback control and oscillatory gene expression on cellular differentiation as shown in 1.3 motivated our lab to mathematically model this gene regulatory network and study their feedback mechanisms in more detail.

1.5 The BMP Regulatory Network

The maturation of the cardiovascular system is a crucial event for a normal embryonic development. There are two distinct forms of vascular formation in the embryo: vasculogenesis and angiogenesis. Vasculogenesis gives rise to the heart and vascular plexus while angiogenesis is responsible for the remodeling of the vascular network and wound healing. Angiogenesis itself consists of two different mechanisms: endothelial sprouting and intussusceptive microvascular growth (IMG)([46]). In general, the growth of blood vessels during embryogenesis is tightly controlled. Angiogenesis is found to be controlled by several soluble growth factors ([66],[48]) such as type-I receptor activin receptor-like kinase 1 (ALK-1) of the transforming growth factor- β (TGF- β) superfamily. Its co-receptor endoglin also plays an important role in angiogenesis and vascular development.

Bone morphogenetic proteins (BMPs) belong to the TGF- β superfamily that are identified for their ability to regulate cell growth, differentiation, cartilage formation, ectopic bone growth, and apoptosis of various cell types. Our collaborators in Dr. Kristina Bostrom's lab at UCLA are specifically interested in investigating this family for their critical role in morphogenesis and differentiation of tissues and organs ([61],[65],[30],[23]). They have previously investigated pattern formation created by the interaction of a protein in this family, specifically BMP-2 and its inhibitor matrix carboxyglutamic acid protein (MGP), which is a small molecule.

Our lab has previously constructed a mathematical model of vascular mesenchymal cells pattern formation based on the interaction of BMP-2 and MGP in the experimental preparations of Dr. Bostrom's Lab at UCLA. The previously constructed mathematical model was a system of partial differential equations over a 2D domain ([28]). This mathematical model predicted spatial pattern formation in different patterns such as stripes, spots, and stripe-doubling. Predictions were validated in an in-vitro vascular mesenchymal cell culture by Dr. Bostrom's lab. Numerical simulations and cell cultures are both shown in 1.5 and 1.4. This mathematical model provided an insight into how the kinetic interaction of these two

chemicals can produce very specific patterns. This was clinically significant because during embryogenesis, mesenchymal stem cells aggregate and organize into patterned tissues. Later in life, when these mesenchymal cells organize into ectopic bone or vascular calcification in tissue, this process can lead to pathological creation of atherosclerotic lesions within the artery wall ([28]).

1.6 Simplified BMP Network Diagram of the Mathematical Model

We have investigated the oscillatory gene expression of the following network shown in figure 1.6 through mathematical modeling and numerical simulations. Specifically, the protein interactions studied in our model involve BMP-9, BMP-4, Endoglin, MGP, CV-2, and ALK-1. BMP-9 is a protein produced by the liver ([13],[14],[40]) that induces the differentiation of mesenchymal cells into cartilage([33]). BMP-9 specifically inhibits basic fibroblast growth factor (bFGF) stimulated proliferation and blocks vascular endothelial growth factor (VEGF) induced angiogenesis ([51]). BMP-9 has been shown to bind with high affinity to the extracellular domain of activin receptor-like kinase 1 (ALK-1) ([13]). ALK-1 is predominantly expressed in endothelial cells and has been shown to regulate EC proliferation and angiogenesis ([53]). Urness et al., 2000 ([62]), have shown that ALK-1 deficient mice were not able to undergo vascular remodeling and angiogenesis ([43], [62]). Endoglin is a co-receptor that forms a complex with ALK-1 to promote the effects of ALK-1 on ECs ([10], [29], [36]). Two pieces of evidence have particularly shown that endoglin plays an essential role on inducing angiogenesis in ALK-1 signal. First, Li et al., 1999 ([38]), have shown that endoglin deficient mice have significantly similar phenotypes as ALK-1 deficient mice. Second, vascular disorder hereditary hemorrhagic telangiectasia (HHT or Osler-Weber-Rendu disease) have been observed in both ALK-1 and endoglin knock out mice. HHT is an autosomal dominant vascular dysplasia that is mainly characterized by arteriovenous malformations in the brain, the lungs, and the liver. Specifically, the ALK-1 mutation is responsible for HHT2, whereas the endoglin mutation is responsible for HHT1 ([32], [39]). Nonetheless, patients with both types of HHT have very similar symptoms with slight differences in the severity of

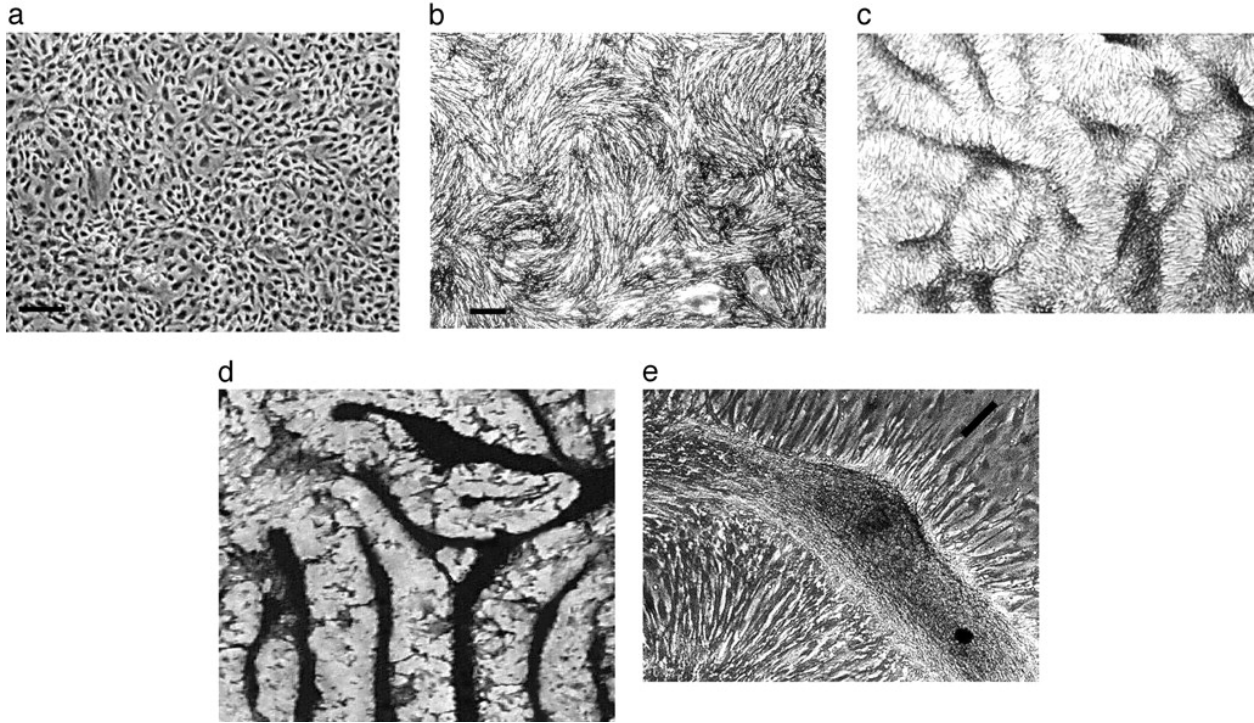


Figure 1.4: A pattern formation in cultured VMCs in vitro. Over 20 days, VMCs plated in vitro develop from a monolayer of randomly oriented cells of nearly uniform density (approximately day 1; stage 1) (a), to local alignment of cells into regions (swirls) of nearly uniform size (approximately day 4; stage 2) (b), to ridges of high cell density (dark areas) (approximately day 10; stage 3) (c), to connected ridges forming a labyrinthine pattern (approximately day 16; stage 4) (von Kossa stain) (d). (e) At 3 higher magnification, a phase-contrast image of an unstained ridge shows the perpendicular orientation of cells in the monolayer relative to the edges of the multicellular ridge. [Bar = 250 μ m (a and b); c and d are at the same magnification as b; bar in e shows the approximate size, shape, and orientation of a single cell ([28]).

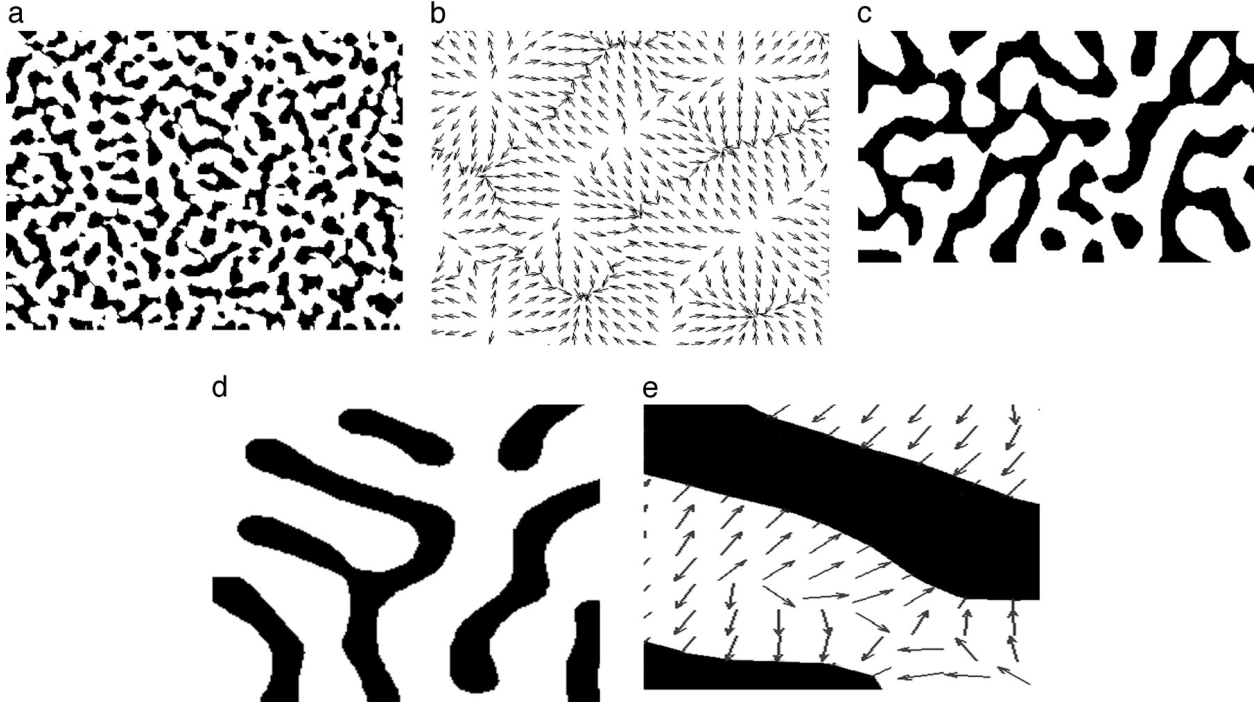


Figure 1.5: Numerical solutions of the mathematical model corresponding to each of the stages from figure 1.4 ([28]).

lung arteriovenous malformations (AVMs). Particularly, people with HHT1 are more likely to have lung AVMs than those with HHT2 ([1]). BMP-4 opposes the action of BMP-9 by stimulating the differentiation of human embryonic stem cells to vascular progenitor cells through Smad signaling and by inducing bFGF stimulated proliferation and VEGF induced angiogenesis ([12], [6], [51]).

BMP-9 and BMP-4 interact with each other through ALK-1. BMP-4 induces ALK-1 expression and BMP-9 binds to ALK-1 as a ligand along with its co-receptor endoglin ([26]). The expression of BMPs mentioned so far are regulated through specific inhibitors that create multiple negative feedback loops. MGP is induced by BMP-9/ALK-1 signaling and inhibits the activity of BMP-4. Since BMP-4 is pro-angiogenesis, inhibition by MGP antagonizes angiogenesis, and MGP knockouts like the ALK-1 knockout lead to AVMs ([60], [68]). CV-2 expression is also induced by BMP-9/ALK-1 signaling. It specifically binds to BMP-9 and inhibits it. Since BMP-9 inhibits angiogenesis and increases EC differentiation,

CV-2 antagonizes EC differentiation and is an angiogenic. Studies have shown that CV-2 knockouts have abnormal vascular endothelium with increased levels of EC differentiation markers ([68]).

1.7 Motivation

Previous mathematical models of the BMP network published by our lab [28] focused on the spatio-temporal dynamics of the model in order to capture pattern formation seen in the cultures. In order to that, partial differential equations were used over a 2D domain. Our current model of the BMP network involves more players along with time-delays. As a result, we designed a mathematical model of the BMP network in vascular endothelial cells through ordinary differential equations with time-delays. The role of temporal fluctuations in this system motivated us to explore the conditions leading to these interesting molecular dynamics and time-delays. In conjunction with our experimental results, we have predicted that oscillatory dynamics of the system correspond to the progenitor state of the endothelial cells, whereas, non-oscillatory dynamics and steady states correspond to the differentiation of mesenchymal stem cells into mature endothelial cells.

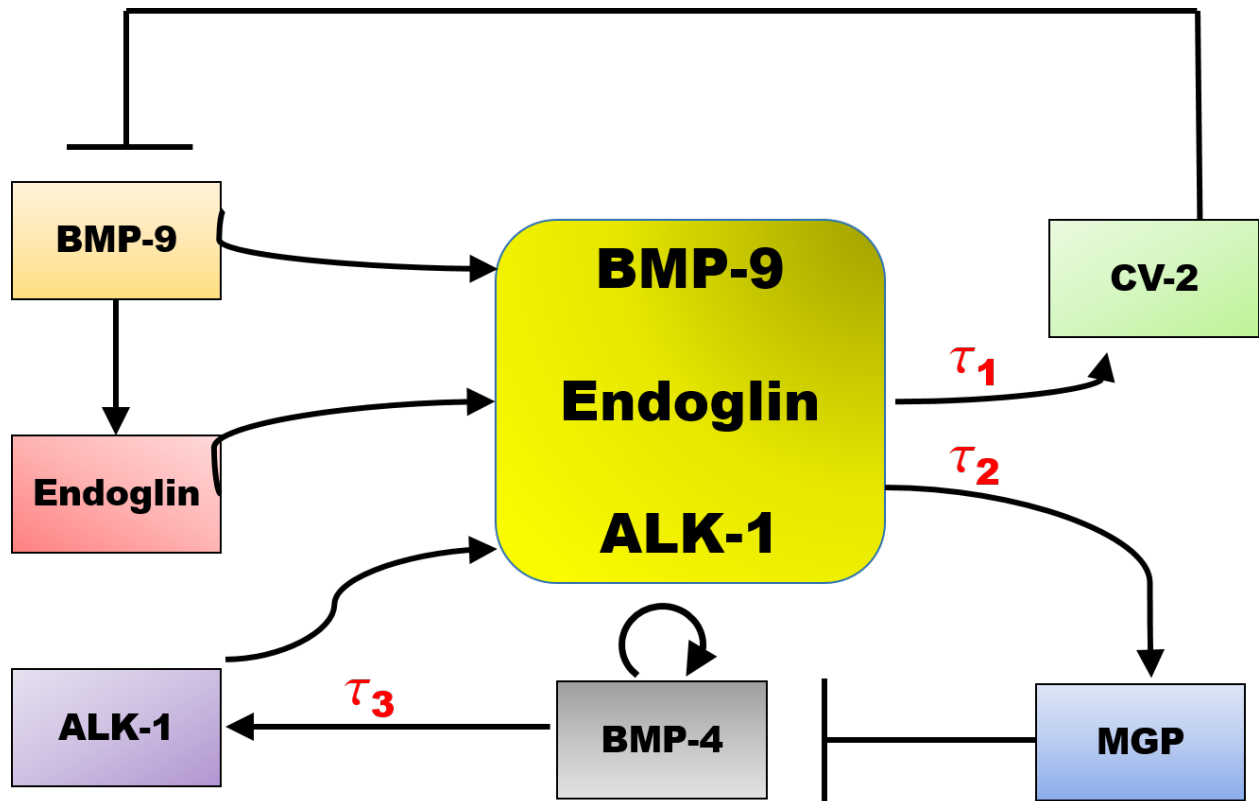


Figure 1.6: **BMP Network Diagram:** Network diagram for biological relationship accounted for in the model. BMP-9 endogenous ligands bind to ALK-1 receptor along with its co-receptor endoglin to stimulate production of CV-2 and MGP with a transcriptional time delay of τ_1 and τ_2 respectively. CV-2 and MGP bind and inhibit BMP-9 and BMP-4, respectively. BMP-4 autocatalytically produces itself and activates ALK-1 transcription with a time delay of τ_3 . BMP-4 signaling is associated with EC progenitor state and it is angiogenic, while BMP-9/ALK-1 signaling stimulates EC differentiation and it is anti-angiogenic.

CHAPTER 2

Methods

2.1 The Non-Linear Time Delay Mathematical Model

We developed a mathematical model of the BMP regulatory network. The model consists of 6 variables with 6 ordinary differential equations, each representing a different protein concentration that are modeled with non linear time-delay ordinary differential equations. The equations model the rate of change of concentrations over time $\frac{ng}{ml.hr}$. The reaction terms are modeled by the interaction of BMP-9, BMP-4, Endoglin, MGP, CV-2, and ALK-1.

The first equation belongs to **BMP-9**, shown below (2.7). The variable A is the concentration of BMP-9 in $\frac{ng}{ml}$. BMP-9 is produced by hepatic biliary cells and is present in the human plasma concentration of 2-12 $\frac{ng}{ml}$ ([20]). k_1 is the source term which represents the constant production rate of BMP-9 in $\frac{ng}{mlhr}$. As mentioned above, BMP-9 is an EC differentiation marker and CV-2 inhibits EC differentiation signaling by inhibiting BMP-9. The inhibitory interaction of CV-2 and BMP-9 is modeled by the CV-2 variable C, which is subtracted from the equation. $\sigma_1 AC$ term represents the inhibition of BMP-9 through CV-2 with σ_1 representing the binding rate of BMP-9 and CV-2 measured in $\frac{ml}{nghr}$. BMP-9 is removed from the system at a rate proportional to its concentration, μ_1 , which is measured in $\frac{1}{hr}$.

$$\text{BMP-9: } \frac{dA}{dt} = k_1 - \sigma_1 AC - \mu_1 A \quad (2.1)$$

The second equation belongs to **BMP-4**, shown below (2.8). The variable B is the concentration of BMP-4 in $\frac{ng}{ml}$. k_2 is the source term which represents the constant production rate of BMP-4 in $\frac{ng}{mlhr}$. BMP-4 is regulated and produced autocatalytically and the squared term in the sigmoidal function is representative of that ([52]). Parameter q is the saturation coefficient of BMP-4 which is induced autocatalytically. In addition, BMP-4 is directly inhibited by MGP, which is represented by the variable M ([68]). The inhibitory interaction of MGP and BMP-4 is modeled by the MGP variable M which is subtracted from the equation. The $\sigma_2 BM$ term represents the inhibition of BMP-4 through MGP with σ_2 as the binding rate of MGP and BMP-4 measured in $\frac{ml}{nghr}$. BMP-4 is removed from the system at a rate proportional to its concentration, μ_2 , which is measured in $\frac{1}{hr}$.

$$\text{BMP-4:} \quad \frac{dB}{dt} = \frac{k_2 B^2}{(1 + q^2 B^2)} - \sigma_2 BM - \mu_2 B \quad (2.2)$$

The third equation belongs to **Endoglin**, shown below (2.9). The variable E is the concentration of Endoglin in $\frac{ng}{ml}$. Endoglin is an auxillary membrane receptor of TGF- β , where it modulates angiogenesis through ALK-1 signaling. BMP-9 inhibits angiogenesis via ALK-1, which makes endoglin a promising target for anti-angiogenic cancer therapy. Specifically, the ALK-1 signaling defects that signal through SMAD-1 lead to a clinically similar form of HHT as described earlier ([32]). This suggests that Endoglin and ALK-1 are in the same signaling pathway. Another piece of evidence that suggests this comes from Panchenko et al. 1996 ([45]) and Roelen et al., 1997 ([49]), which shows a very similar expression pattern of ALK-1 and Endoglin in the vascular endothelium. It has been shown that TGF- β signaling via SMAD transcription factors stimulates endoglin expression, in which BMP-9 specifically stimulates the production of endoglin as shown in our BMP Network Diagram (1.6) ([11], [35],[50],[55]). k_3 is the source term and maximal releasable amount of endoglin and represents the constant production rate of endoglin in $\frac{ng}{mlhr}$. Endoglin stimulation by BMP-9 is modeled by a sigmoidal function to capture its saturation dynamics when the concentration of endoglin is elevated, since endoglin cannot be exponentially induced by BMP-9. Endoglin

is removed from the system at a rate proportional to its concentration, μ_3 , which is measured in $\frac{1}{hr}$.

$$\text{Endoglin:} \quad \frac{dE}{dt} = \frac{k_3 A^2}{(1 + \rho^2 A^2)} - \mu_3 E \quad (2.3)$$

The fourth equation belongs to **MGP**, shown below (2.10). The variable M is the concentration of MGP in $\frac{ng}{ml}$. k_4 is the source term which represents the constant production rate of MGP in $\frac{ng}{mlhr}$. MGP is produced as a downstream product of BMP-9/ALK-1/Endoglin signaling. Previous data from Dr. Bostrom's Lab at UCLA have shown that MGP is over-expressed with a time delay after the treatment of human aortic endothelial cells (HAECs) with BMP-9 ([68]). Since ALK-1 is the preferred bound receptor for BMP-9 and endoglin is its co-receptor, the MGP equation is modeled with all three of them along with time delay. MGP is removed by the system when it binds to BMP-4. The term $\sigma_2 BM$ represents this removal, since after binding MGP is no longer available to act in the system. MGP is also removed from the system at a rate proportional to its concentration, μ_4 , which is measured in $\frac{1}{hr}$.

$$\text{MGP:} \quad \frac{dM}{dt} = k_4 A(t - \tau_1) S(t - \tau_1) E(t - \tau_1) - \sigma_2 BM - \mu_4 M \quad (2.4)$$

The fifth equation belongs to **CV-2**, shown below (2.11). CV-2 is another inhibitory molecule making the multiple negative feedback loop in the system. It is modeled by the variable C, which is the concentration of CV-2 in $\frac{ng}{ml}$. k_5 is the source term which represents the constant production rate of CV-2 in $\frac{ng}{mlhr}$. CV-2 production is also downstream of BMP-9/ALK-1/Endoglin signaling similar to MGP, and it was found by Dr. Bostrom's Lab that its expression peaks with a time delay after the treatment of HAECs with BMP-9 ([68]). As a result, the CV-2 is modeled by the same reasoning as MGP with a different time delay. CV-2 is removed by the system when it binds to BMP-9. The term $\sigma_1 AC$ represents this

removal, since after binding CV-2 is no longer available to act in the system. CV-2 is also removed from the system at a rate proportional to its concentration, μ_5 , which is measured in $\frac{1}{hr}$.

$$\text{CV-2: } \frac{dC}{dt} = k_5 A(t - \tau_2) S(t - \tau_2) E(t - \tau_2) - \sigma_1 AC - \mu_5 C \quad (2.5)$$

The sixth equation belongs to **ALK-1**, shown below (2.12). ALK-1, the preferred receptor of BMP-9, is modeled by the variable S which is the concentration of ALK-1 in $\frac{ng}{ml}$. BMP-4 stimulates the expression of ALK-1 ([54]). It has been shown that ALK-1 expression also peaks with a time delay after treating the HAECs with BMP-4 ([68]). k_6 is the source term which represents the constant production rate of ALK-1 in $\frac{ng}{mlhr}$. The induction of ALK-1 by BMP-4 with a time delay is modeled with the term $k_6(B(t - \tau_3))^2$. ALK-1 removal from the system occurs primarily through endocytosis from the plasma membrane. ALK-1 is removed from the system at a rate proportional to its concentration, μ_6 , which is measured in $\frac{1}{hr}$.

$$\text{ALK-1: } \frac{dS}{dt} = k_6((B(t - \tau_3)))^2 - \mu_6 S \quad (2.6)$$

2.2 BMP ODE System

All six equations are shown below as a system:

$$\text{BMP-9: } \frac{dA}{dt} = k_1 - \sigma_1 AC - \mu_1 A \quad (2.7)$$

$$\text{BMP-4:} \quad \frac{dB}{dt} = \frac{k_2 B^2}{(1 + q^2 B^2)} - \sigma_2 BM - \mu_2 B \quad (2.8)$$

$$\text{Endoglin:} \quad \frac{dE}{dt} = \frac{k_3 A^2}{(1 + \rho^2 A^2)} - \mu_3 E \quad (2.9)$$

$$\text{MGP:} \quad \frac{dM}{dt} = k_4 A(t - \tau_1) S(t - \tau_1) E(t - \tau_1) - \sigma_2 BM - \mu_4 M \quad (2.10)$$

$$\text{CV-2:} \quad \frac{dC}{dt} = k_5 A(t - \tau_2) S(t - \tau_2) E(t - \tau_2) - \sigma_1 AC - \mu_5 C \quad (2.11)$$

$$\text{ALK-1:} \quad \frac{dS}{dt} = k_6 ((B(t - \tau_3)))^2 - \mu_6 S \quad (2.12)$$

2.3 Parameter Estimation

Practically speaking, parameter estimation is one of the toughest problems in dynamical systems modeling with many resources, such as research review articles devoted to this area ([4],[7],[8],[16]). In general, parameter estimation is based on numerical analysis, probability and statistical inference, and theory. In our model, we used experimental results of gene expression analysis on cell cultures of HPAECs done in Dr. Bostrom's lab at UCLA in order to estimate some of the production rates and degradation rates. All parameters estimated are shown in table 2.1.

2.3.1 Production Rates

In a set of experiments, the HPAEC culture was treated with $50 \frac{ng}{ml}$ of BMP-4, and expression of ALK-1 and BMP-9 were measured. In an unpublished work, a member of our lab estimated the production rates of BMP-9 and BMP-4 ([69]), which estimated $k_2=10$. Similarly, k_1 , the production rate of BMP-9, was estimated to be 5 based on its human vascular circulation ([20], [69]). In another set of experiments, fold changes of mRNA expression of Endoglin, MGP, CV-2, and ALK-1 were measured, and the magnitude of expression levels was about 5-10 fold lower than BMP-9 and BMP-4. We conservatively approximated these production rate values to be 1 based on the production rates of BMP-9 and BMP-4 estimated from Dr. Bostrom's lab's experiments ([69]).

2.3.2 Degradation Rates

The upper limit of proteolytic degradation of the BMP-2 and its homologs is 5 percent of its production rate ([24]). BMP-4 autocatalytic dynamics is very similar to BMP-2 that was previously modeled by our lab ([28]). We estimated BMP-4 degradation rate as 15 percent of its production rate, because we also considered its degradation by other routes, like sequestration into extracellular matrix ([70]). The rest of the degradation rate parameters were estimated to be 60 percent of their production rates. These degradation rate parameters are crucial to the system's behavior and will be altered in our simulation experiments.

Based on unpublished work, it was observed that MGP is taken up more avidly by the extracellular matrix than BMP-2 ([28]), and the rest of the variables in the system had similar magnitude to MGP expression levels. Therefore, we estimated their degradation rates to be 60 percent of their production rates due to extensive degradation by other routes. It was previously observed based on the experimental results that the BMP-4 degradation rate has to be lower than the rest of the system's degradation rates in order to capture the oscillatory

dynamics in the cell cultures.

2.3.3 Time Delays and Coefficients

We estimated the time delays of our system based on the mRNA expression data from HPAECs. MGP and CV-2 transcriptional delays are about 7 hours apart and CV-2 takes 7 hours longer after MGP, so we estimated their time delays respectively to be 13 and 20 hours. ALK-1 transcription time delay was also estimated from the experimental data to be 8 hours.

q is the BMP-4 saturation coefficient and it was estimated based on a previous paper published by our lab, ([15]). In that paper, Chen et al., 2012, studied a biological model of cultured vascular mesenchymal cells (VMCs) that self organize into aggregates. BMP-4 autocatalytic saturation coefficient was estimated from the experiments and it is shown in figure 3 of that paper. The saturation coefficient is to the power of 2. As a result, q is $\sqrt{5}$.

A similar experiment was recently done by Dr. Bostrom's lab for endoglin and the endoglin saturation coefficient, ρ , was estimated to be $\sqrt{2.5}$. This was determined after fitting a sigmoidal curve to the data representing the fold expression increase of endoglin with different concentrations of BMP-9, since endoglin is induced by BMP-9. As a result, ρ is $\sqrt{2.5}$.

σ_1 is the inhibition rate of CV-2 on BMP-9. Based on experimental data, it was observed that CV-2 is an extremely potent inhibitor of BMP-9. As a result, the rate was estimated to be 1, meaning that every time a molecule of CV-2 interacts with a molecule of BMP-9, the inhibition occurs. This makes the inhibition success rate to be 100 percent. Furthermore, σ_2 is the inhibition rate of MGP on BMP-4. Danino et al., 2011 ([19]), have estimated the lower limit of the inhibition rate of MGP on BMP-2 to be $0.2 \frac{ml}{ng hr}$. Based on the similar dynamics

of BMP-2 and BMP-4, we conservatively chose the inhibition rate of MGP on BMP-4 to be this lower limit, $\sigma_2=0.2 \frac{ml}{nghr}$.

2.4 Stability, Equilibrium Points and Steady State Analysis

2.4.1 Numerical Integration Algorithm

We used *Mathematica* software to numerically simulate the set of ODEs with time delays using parameter values describes above in table (2.1). All initial conditions were set to 1, although the system's behavior was not sensitive to these choices.

2.4.2 State Space Geometry

We visualize the motions of state variables in state space. State space is n -dimensional, and in state space geometry, we represent each state variable as an axis in a multi-dimensional Euclidean space. Motion of the states of the system can be drawn in a multi-dimensional state space which yields a state space diagram. We have shown the state space diagrams for our model to define the motion of the system as it evolves through the plane in time from the initial time to the final time specified in the numerical integration algorithm. In case of stable oscillations, a stable limit cycle is shown, which attracts all the neighboring trajectories in order to exhibit sustained oscillations. Limit cycles play an important role in biology and describe many biological rhythms. Our model oscillatory behavior also exhibit limit cycling behaviors. Our model consists of 6 variables, which, by nature, has a 6-D dynamical system trajectories in state space. In order to be able to represent the trajectories, we show two different state space diagrams, each showing 3 different variables. Phase diagrams are similar to state space diagrams, but instead of variables, we represent each parameter as an axis

Table 2.1: Model Parameters: This table contains the approximate values, units and the biological functions of parameters used in this study.

Dimensional Parameters	Value	Units	Function	Source
k_1	5	$\frac{ng}{mlhr}$	BMP-9 Production Rate	2.7
k_2	10	$\frac{ng}{mlhr}$	BMP-4 Production Rate	2.8
k_3	1	$\frac{ng}{mlhr}$	Endoglin Production Rate	2.9
k_4	1	$\frac{ng}{mlhr}$	MGP Production Rate	2.10
k_5	1	$\frac{ng}{mlhr}$	CV-2 Production Rate	2.11
k_6	1	$\frac{ng}{mlhr}$	ALK-1 Production Rate	2.12
μ_1	3	$\frac{1}{hr}$	BMP-9 Degradation Rate	2.7
μ_2	1.5	$\frac{1}{hr}$	BMP-4 Degradation Rate	2.8
μ_3	0.6	$\frac{1}{hr}$	Endoglin Degradation Rate	2.9
μ_4	0.6	$\frac{1}{hr}$	MGP Degradation Rate	2.10
μ_5	0.6	$\frac{1}{hr}$	CV-2 Degradation Rate	2.11
μ_6	0.6	$\frac{1}{hr}$	ALK-1 Degradation Rate	2.12
τ_1	13	hr	MGP Transcriptional Time Delay	2.10
τ_2	20	hr	CV-2 Transcriptional Time Delay	2.11
τ_3	8	hr	ALK-1 Transcriptional Time Delay	2.12
σ_1	1	$\frac{ml}{nghr}$	CV-2 and BMP-9 Binding Rate	2.7 and 2.11
σ_2	0.2	$\frac{ml}{nghr}$	MGP and BMP-4 Binding Rate	2.8 and 2.8
q	$\sqrt{5}$	No unit	BMP-4 Saturation Coefficient	2.8
ρ	$\sqrt{2.5}$	No unit	Endoglin Saturation Coefficient	2.9

in a multi-dimensional Euclidean space. We also use phase diagrams to represent many simulations for our time delay parameters. Each set of time delays shows the behavior of the system.

2.4.3 Equilibrium

Stability of a nonlinear system refers to its behavior at and near system equilibrium points. There are one or more stationary points called steady states that the system approaches to the steady state. When we talk about the stability of a nonlinear system, we talk about the stability of its equilibrium points. Whereas, in most cases that linear systems are discussed, the stability refers to the stability of the ODE model and not its equilibrium points.

We can either have none or more equilibrium points. The question we often ask is: what happens if we perturb the system away from the equilibrium point? For continuous nonlinear ODE systems such as our mathematical model, which is in the form of $\dot{x}(t) = \mathbf{f}(x(t), \mathbf{p}, \mathbf{u}(t))$, the equilibrium points are the points for which all the terms equal zero.

Nonlinear systems generally have multiple equilibria in state space with different stability properties for each equilibrium. In planar geometries, we can perform a qualitative analysis using different initial conditions in order to understand the behavior of the model and its motion through space. In general, the dynamical properties of the system depend upon their initial conditions and parameters. However, as the name suggests, in nonlinear models, the dynamics behave in a nonlinear way based on their inputs and parameters. As a result, it is computationally challenging to pin down all the parameters along with their stability.

Furthermore, delay differential equations (DDEs) differ from ODEs in that the derivative at any time point depends on the solution at prior times. They often arise in biological models when assumptions are more realistic. For example, the birth rate of predators is

affected by the prior number of predators or preys rather than solely on the current number of predators and preys in the current time. Since the derivative is dependent upon the solution at previous times, it is necessary to provide an initial history before time $t=0$. However, DDE equilibrium points are calculated the same as a regular ODE system.

2.5 Oscillation Period Analysis with the Fourier Transform Method

In order to get more insight about how the time delays affect the dynamical behavior of our system, we analyzed the period of oscillations using the Fourier Transform method. Any periodic time series can be expressed as a combination of cosine or sine waves with different periods and amplitudes. This fact is utilized in Fourier analysis to examine the periodic behavior in a time series. We have used a periodogram array to identify the dominant periods of our time series. Our goal was to identify the regions where the times series oscillation period is 24 hours, which might explain the oscillation patterns observed in experimental data. We used *Mathematica* to find the period of oscillation in different regions. We analyzed the system by fixing one of the time delays and changing the other two. The Fourier Transform method was performed from 400 to 1000 time points with step size of 0.1. All time delays are scanned from 0-20 hours in 1 hour intervals.

CHAPTER 3

Results

3.1 System Simulations Using Parameter Estimation Table 2.1

Numerical solutions for the mathematical model developed based on our parameter estimations are shown in this section. Computation and plotting were accomplished with a *Mathematica* script.

3.2 System's Equilibria and Stability

We have calculated the systems' equilibria, and we have found that our system has two stable equilibria vectors.

$$\left(\begin{array}{l} BMP - 9 = 1.41171 \\ BMP - 4 = 0.902407 \\ Endoglin = 0.555227 \\ MGP = 1.39651 \\ CV - 2 = 0.541803 \\ ALK - 1 = 1.39056 \end{array} \right) \quad \text{and} \quad \left(\begin{array}{l} BMP - 9 = 1.64677 \\ BMP - 4 = 0.176264 \\ Endoglin = 0.580973 \\ MGP = 0.128188 \\ CV - 2 = 0.0362439 \\ ALK - 1 = 0.0851148 \end{array} \right)$$

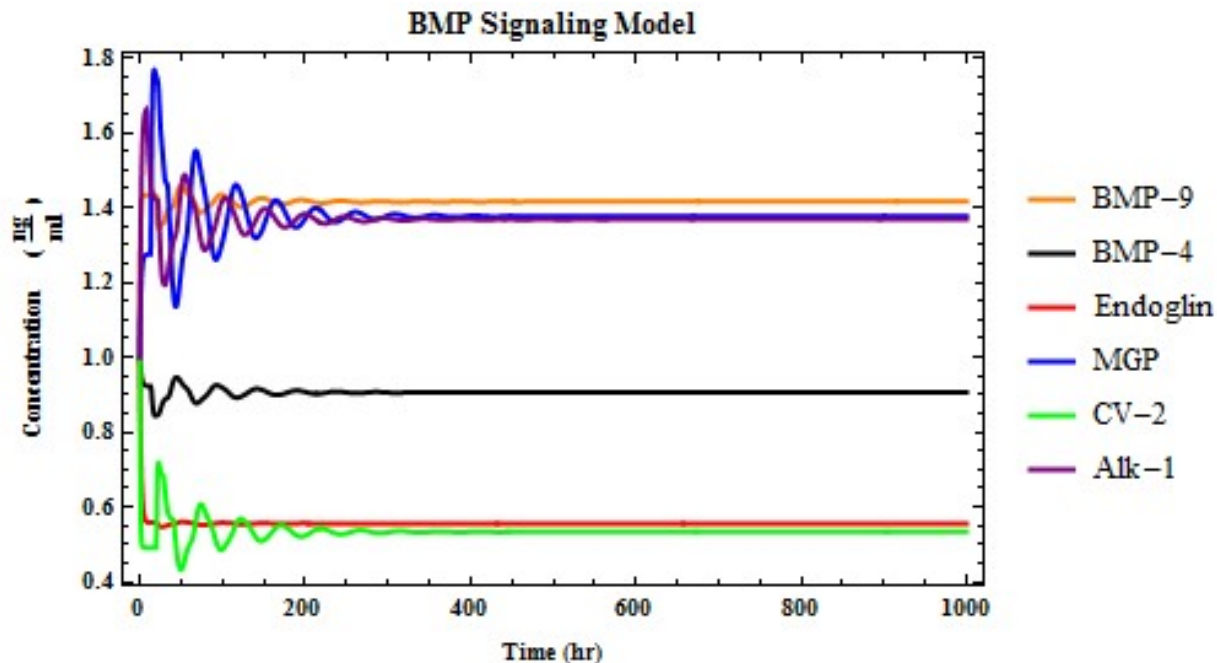


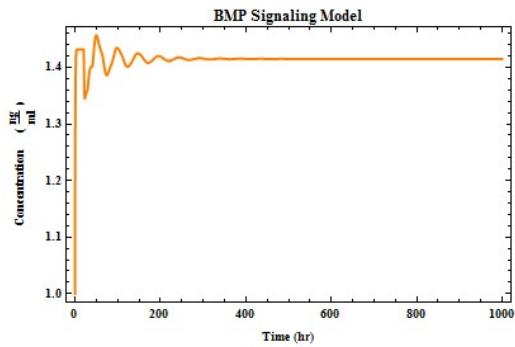
Figure 3.1: Temporal responses for the mathematical model of BMP using the parameter values estimated 2.1 and all initial conditions were set to 1.

3.3 Oscillation Simulation of the Model

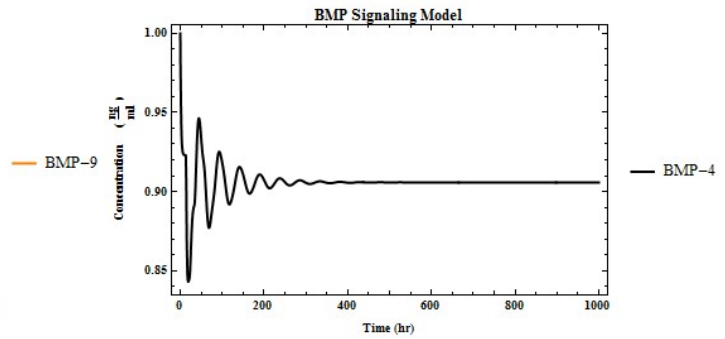
Using a new set of parameters, we obtain sustained oscillations as shown below in figure 3.5 with periods of oscillation around 24 hours with time delays of 4, 11, and 8 hours, respectively, by increasing the degradation rates of Endoglin, MGP, and CV-2 to 80 percent of their production rates and reducing ALK-1 and BMP-9 to 65 and 20 percent of their production rates, respectively.

3.4 Fourier Analysis Results

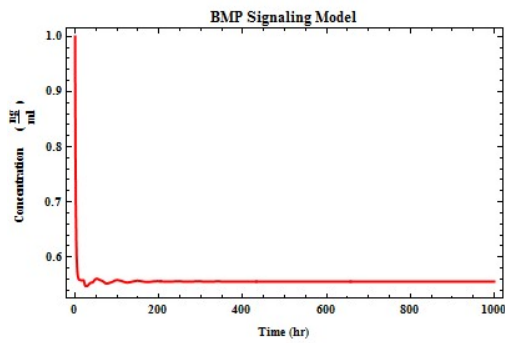
Figures shown below are the phase diagrams using the Fourier Transform method for different time delays. Each variable is presented in a separate figure with three different conditions



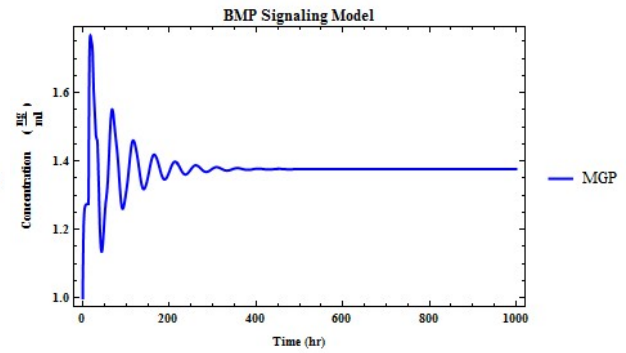
(a) BMP-9



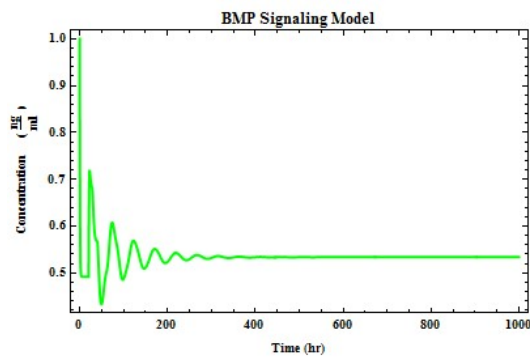
(b) BMP-4



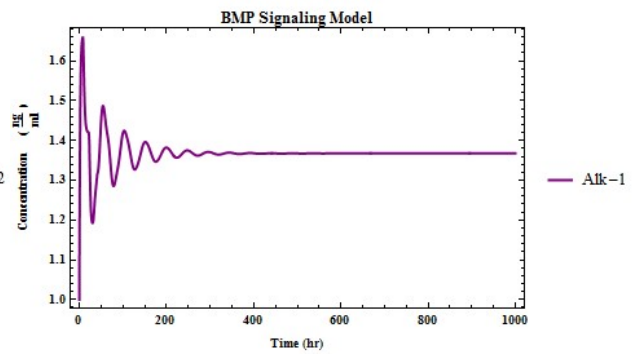
(c) Endoglin



(d) MGP



(e) CV-2



(f) ALK-1

Figure 3.2: Temporal responses for the individual variables in the mathematical model of BMP using the parameter values estimated 2.1 and all initial conditions were set to 1.

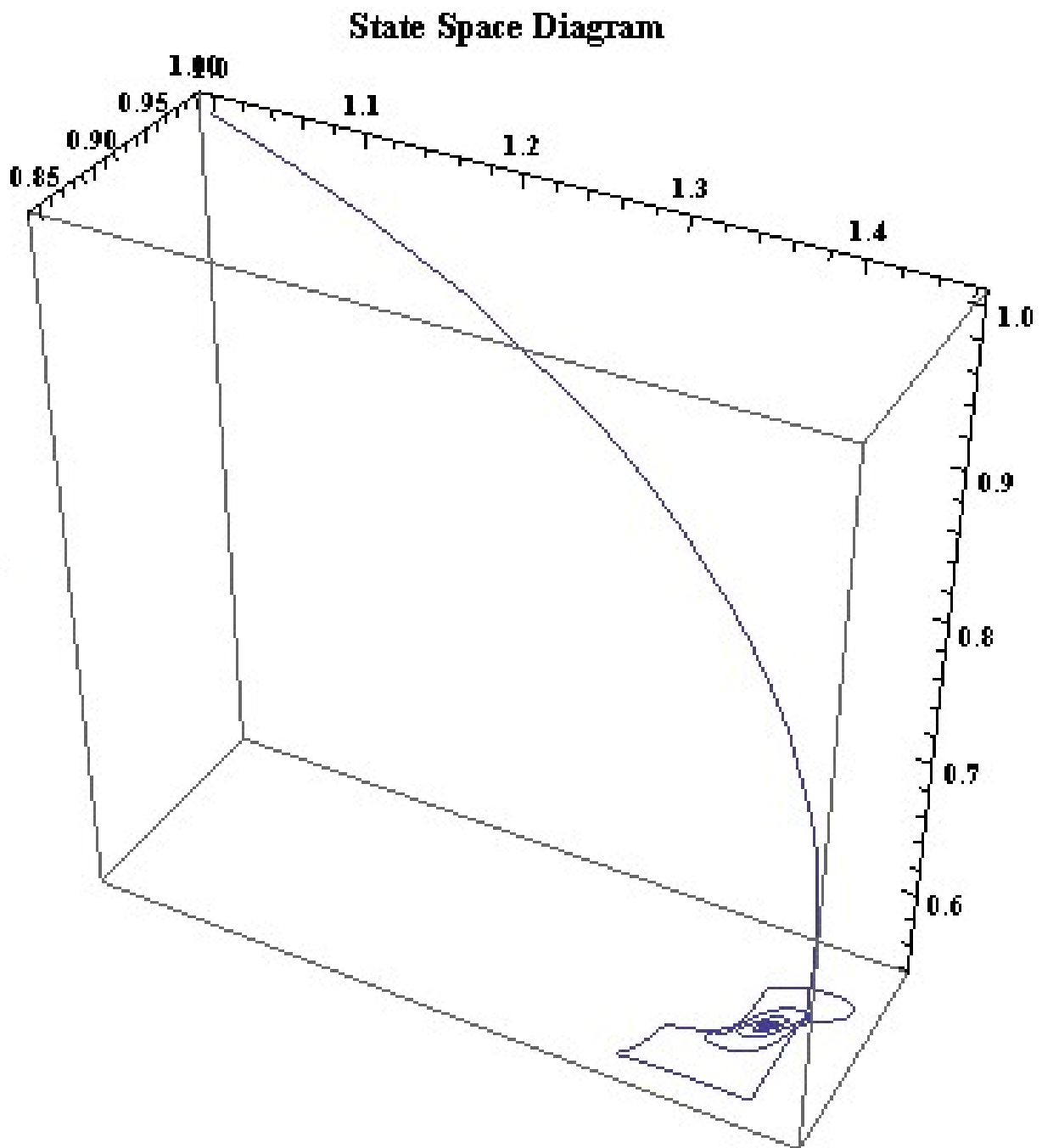


Figure 3.3: **State Space Diagram:** state space solution are illustrated in 3D plot for BMP-9, BMP-4 and Endoglin shown in 3.2.

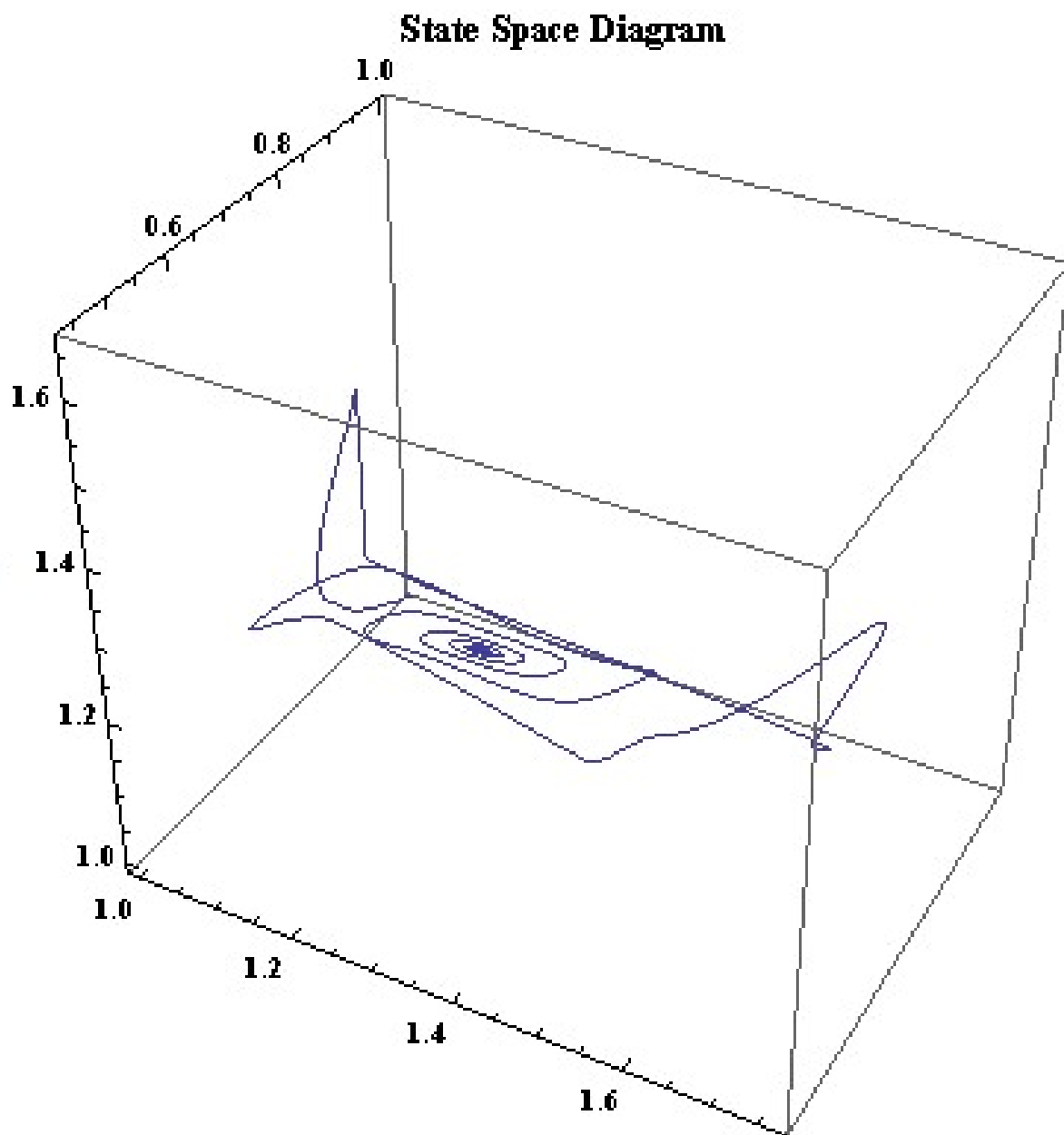


Figure 3.4: **State Space Diagram:** state space solutions are illustrated in 3D plot for MGP, CV-2 and ALK-1 shown in 3.2.

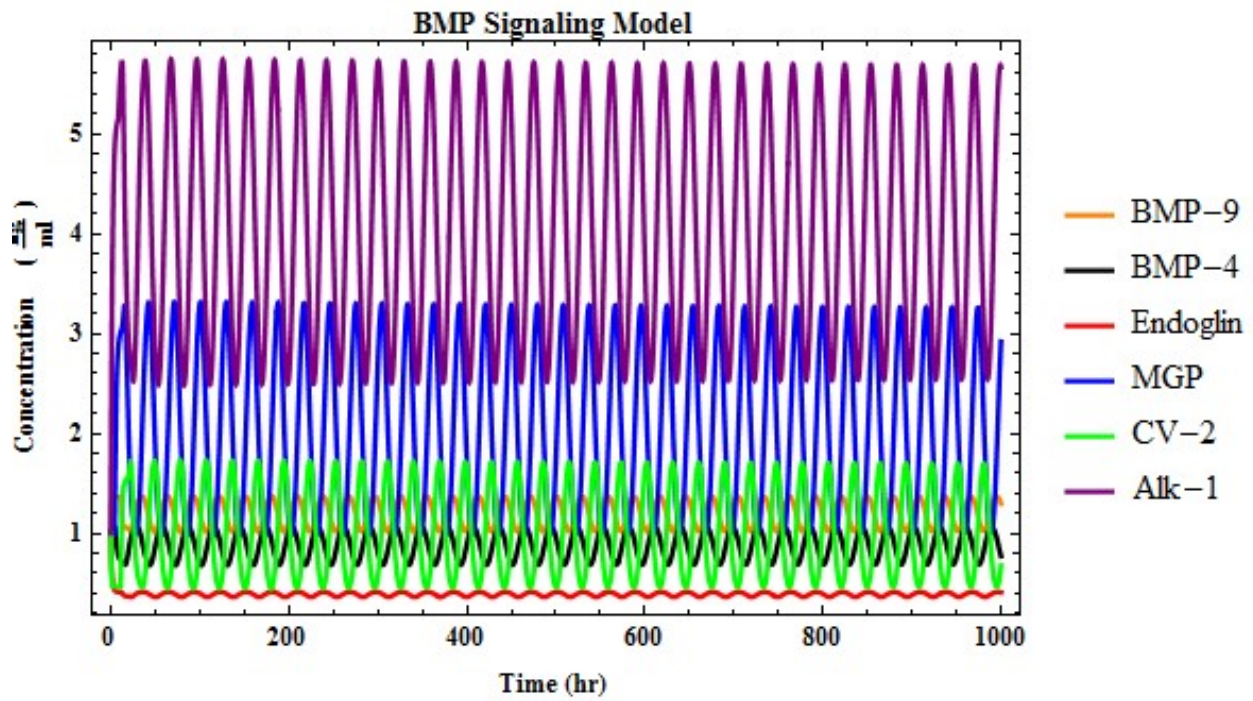
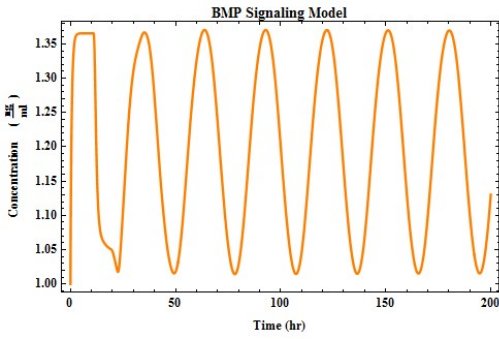
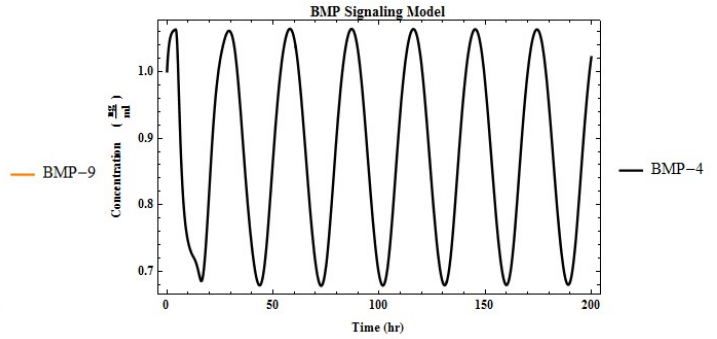


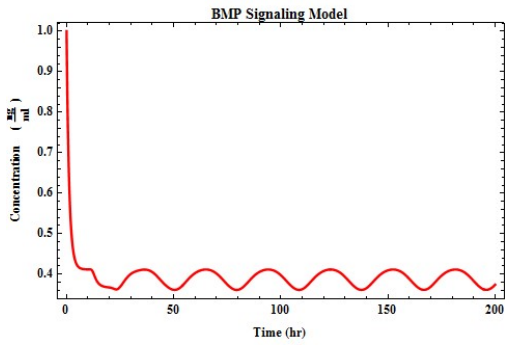
Figure 3.5: **The simulation results of the model:** Temporal responses for the mathematical model of BMP using the parameter values estimated 2.1, but using different degradation rates for BMP-9 at 65 percent, Endoglin, MGP, and CV-2 at 80 percent and ALK-1 at 15 percent of their production rates.



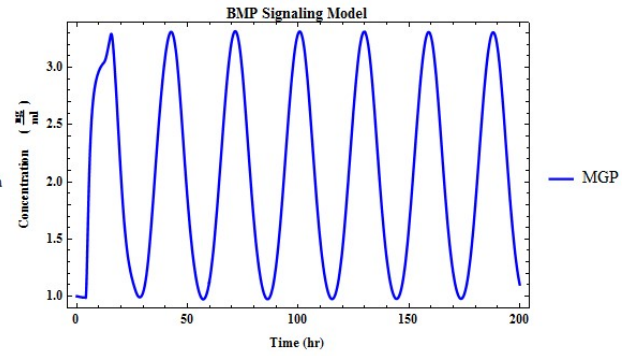
(a) BMP-9



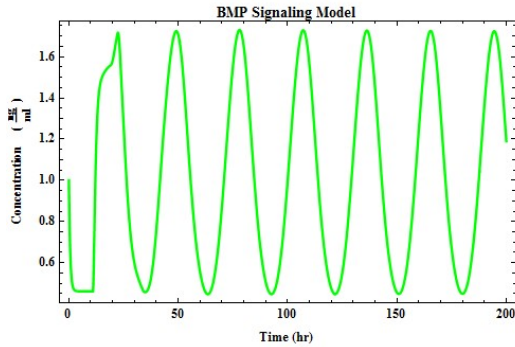
(b) BMP-4



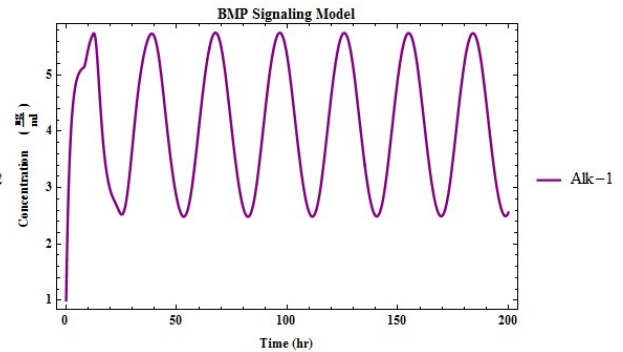
(c) Endoglin



(d) MGP



(e) CV-2



(f) ALK-1

Figure 3.6: **The simulation results of the model:** Temporal responses for the individual variables of BMP using the parameter values estimated 2.1, but using different degradation rates for BMP-9 at 65 percent, Endoglin, MGP, and CV-2 at 80 percent and ALK-1 at 15 percent of their production rates.

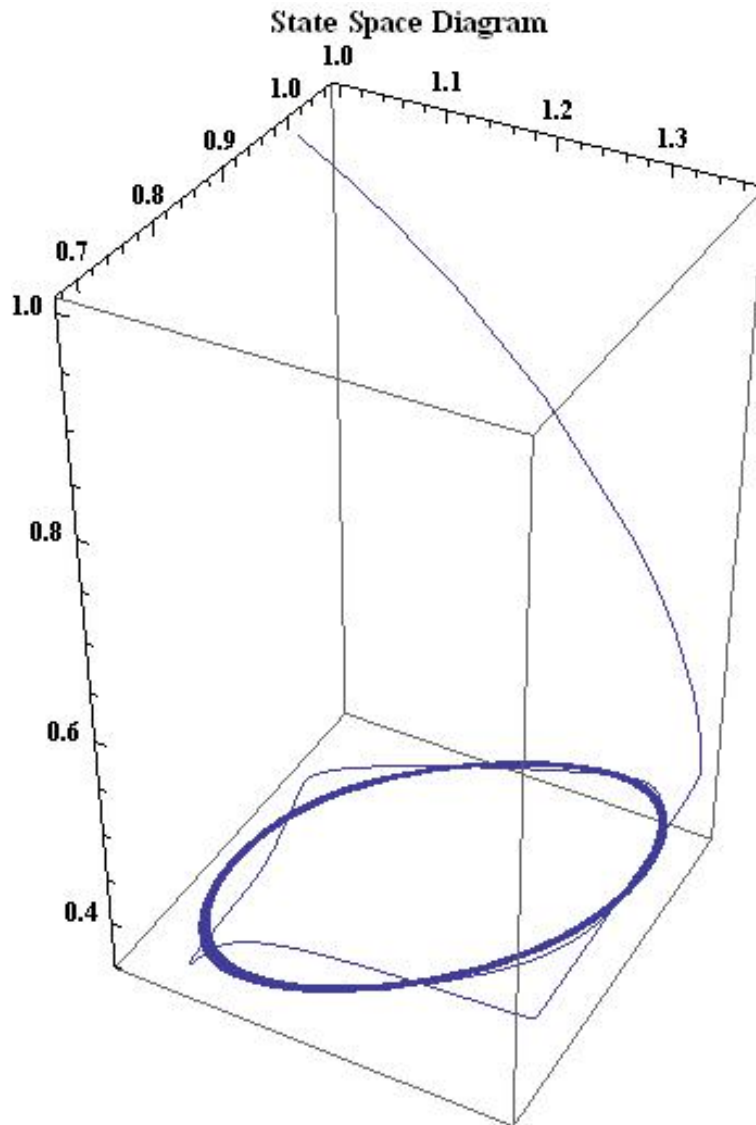


Figure 3.7: **State Space Diagram:** state space solution are illustrated in 3D plot for **BMP-9**, **BMP-4** and **Endoglin** shown in 3.6.

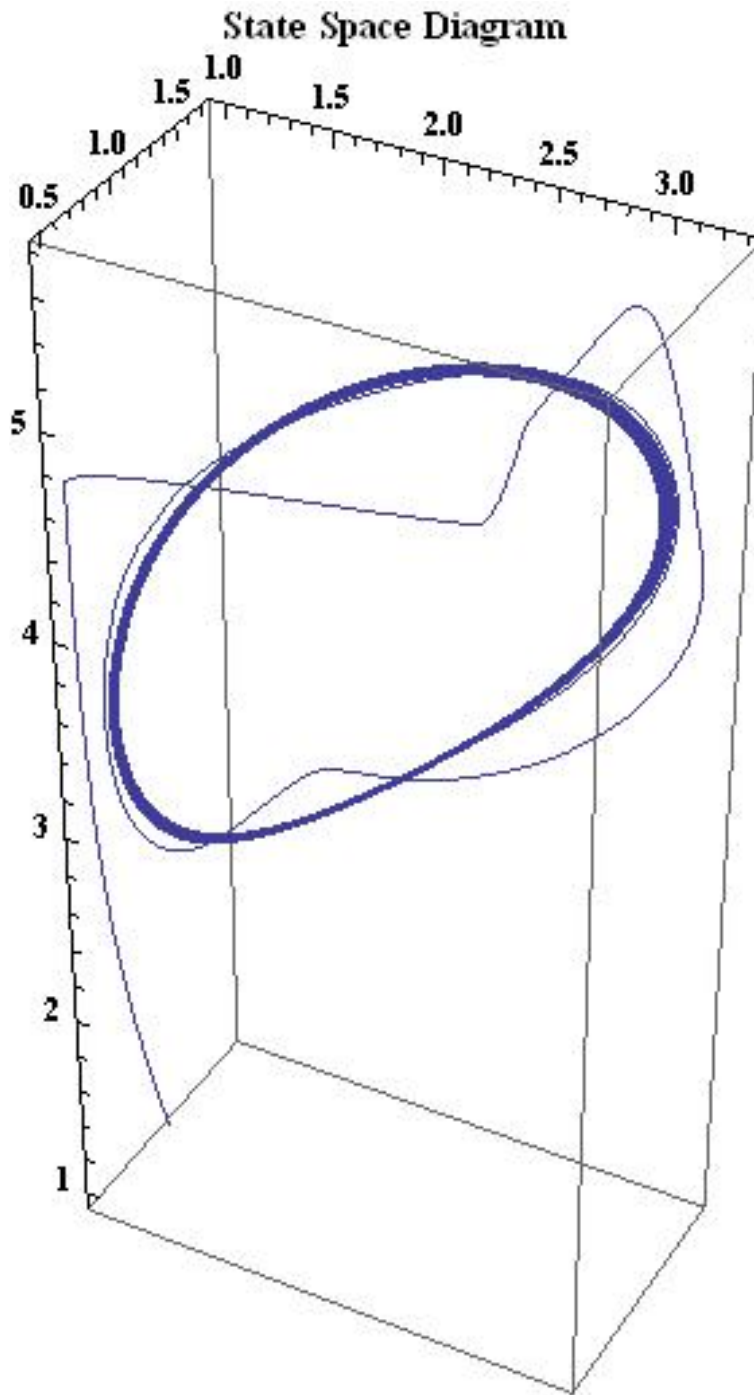


Figure 3.8: **State Space Diagram:** state space solutions are illustrated in 3D plot for MGP, CV-2 and ALK-1 shown in 3.6.

as: τ_1 versus τ_2 , τ_1 versus τ_3 , and τ_2 versus τ_3 while fixing the other τ constant. We studied the mathematical model illustrated above to display oscillatory dynamics using different parameter sets in Fourier Analysis. We first simulated the gene expression levels of this model using the parameter ranges that were investigated in table 2.1, but we obtained damped oscillation. Decreasing the degradation rate of BMP-9 to 40 percent of its production rate while fixing all other parameters produces sustained oscillations, but the oscillatory regimes have periods that are higher than 24 hours. We sought to determine which conditions of parameter values could give rise to the oscillations seen in the biological experiments. We took as a requirement that the oscillations have the following properties:

- $\tau_2 > \tau_1$
- $\tau_2 - \tau_1$ is approximately 7-9 hours.
- τ_3 is approximately 7-10 hours.
- Oscillation period is about 20-27 hours.

Possible combinations of parameters that would give oscillations consistent with the above conditions are the regions specified below:

- $\tau_1 = 1 - 4$ hr, $\tau_2 = 11-15$ hr, $\tau_3 = 8$ hr
- $\tau_1 = 1 - 7$ hr, $\tau_2 = 11$ hr, $\tau_3 = 1 - 8$ hr
- $\tau_1 = 4$ hr , $\tau_2 = 8 - 14$ hr, $\tau_3 = 1 - 8$ hr

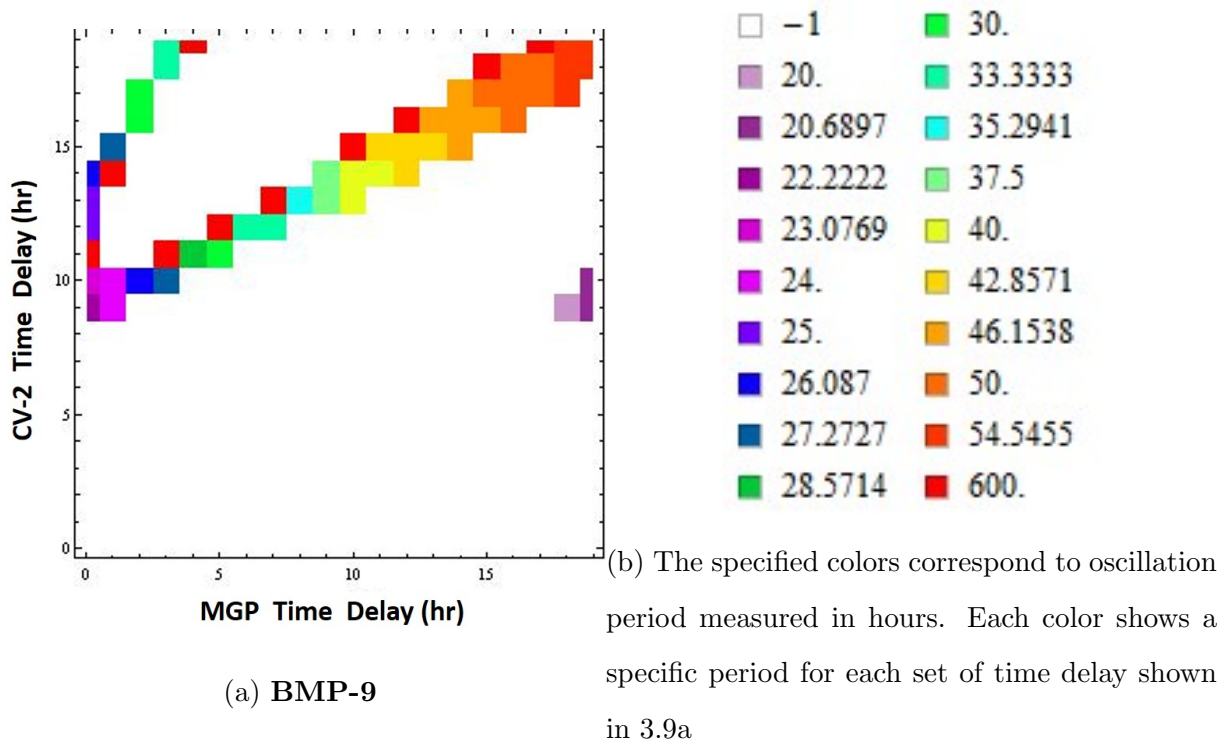


Figure 3.9: **Fourier Analysis of BMP-9:** Oscillation periods are shown with different time delays for MGP and CV-2 transcription while keeping ALK-1 transcriptional time delay constant at 8 hours. All parameters are used from 3.5.

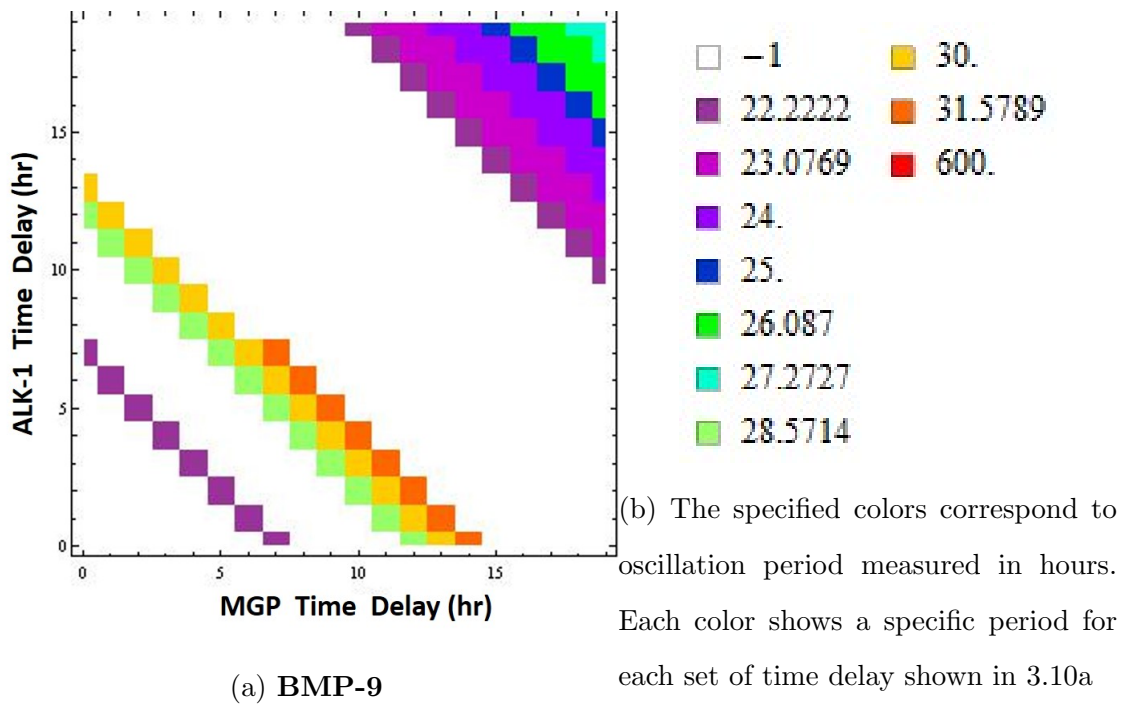


Figure 3.10: **Fourier Analysis of BMP-9:** Oscillation periods are shown with different time delays for MGP and ALK-1 transcription while keeping CV-2 transcriptional time delay constant at 11 hours. All parameters are used from 3.5.

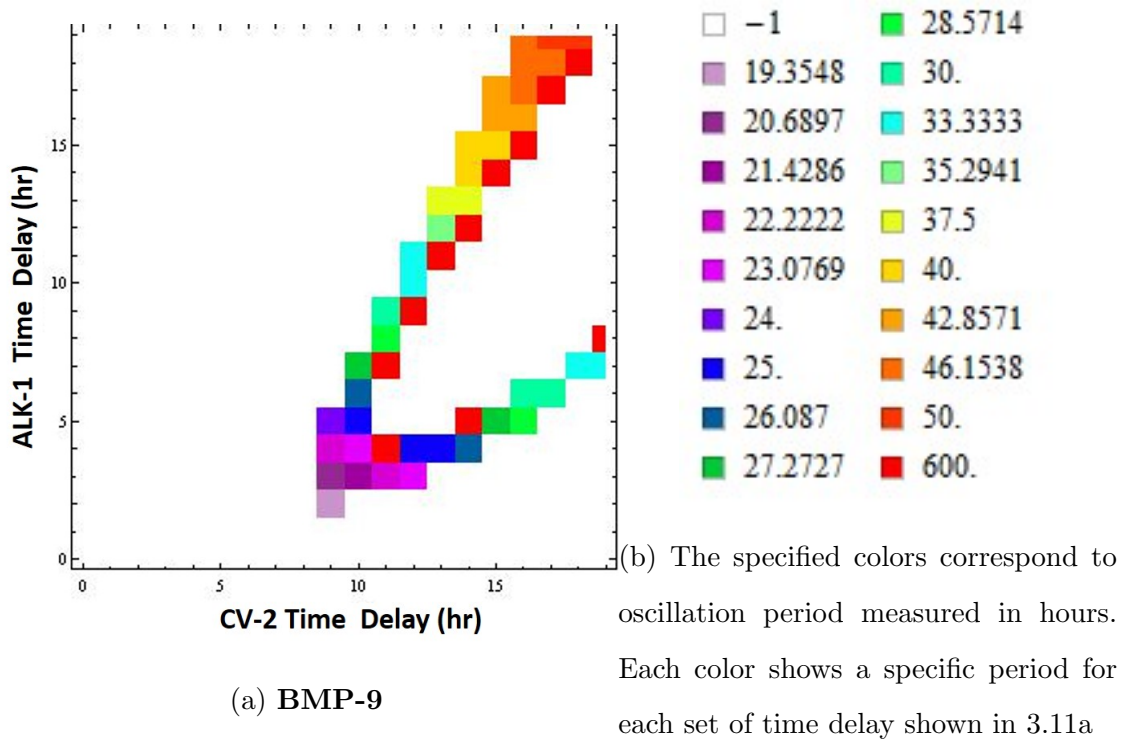
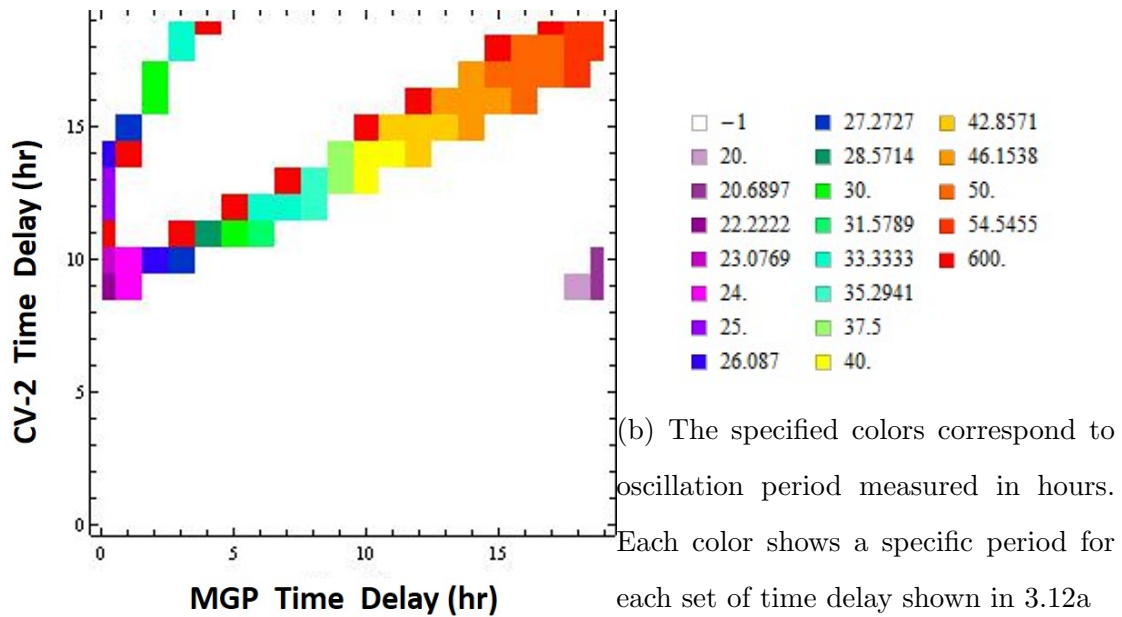


Figure 3.11: **Fourier Analysis of BMP-9:** Oscillation periods are shown with different time delays for CV-2 and ALK-1 transcription while keeping MGP transcriptional time delay constant at 4 hours. All parameters are used from 3.5.



(a) BMP-4

Figure 3.12: **Fourier Analysis of BMP-4:** Oscillation periods are shown with different time delays for MGP and CV-2 transcription while keeping ALK-1 transcriptional time delay constant at 8 hours. All parameters are used from 3.5.

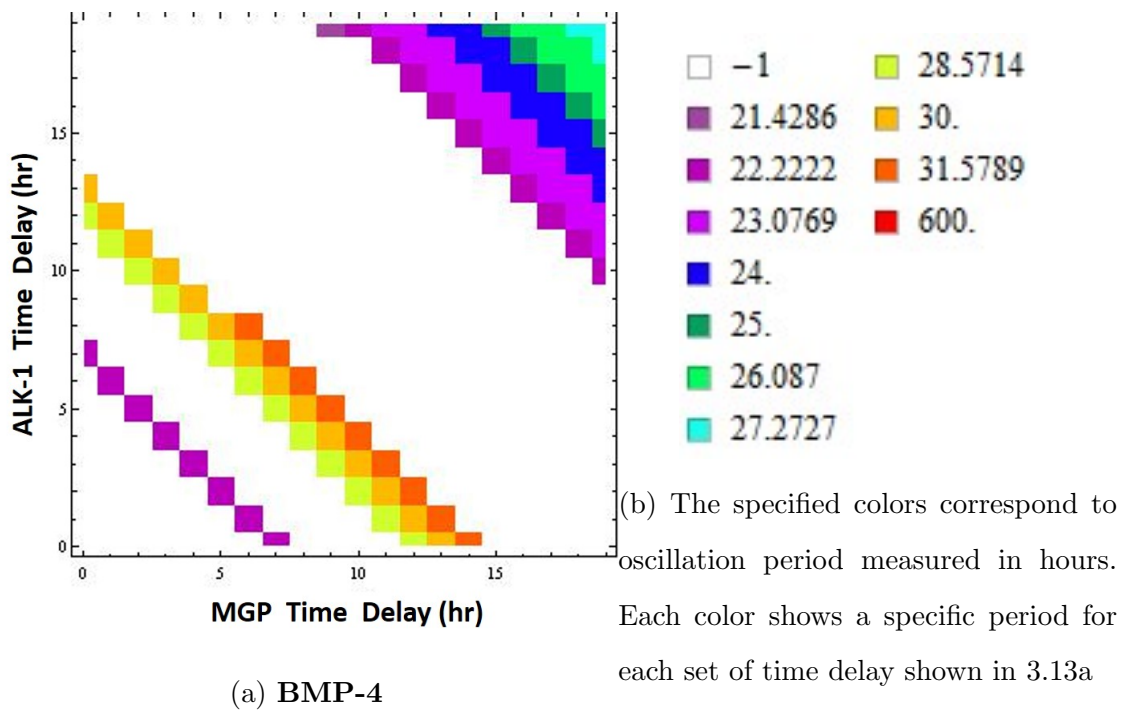
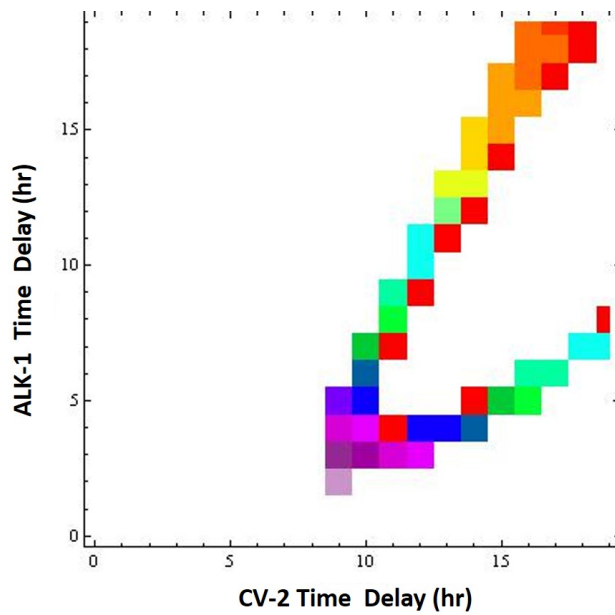
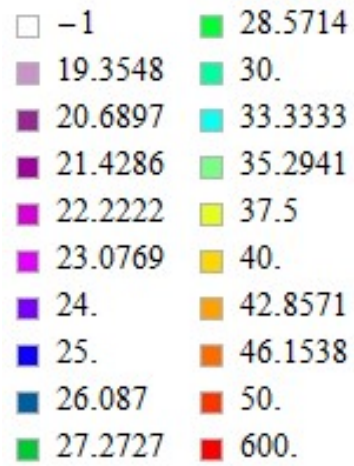


Figure 3.13: **Fourier Analysis of BMP-4:** Oscillation periods are shown with different time delays for MGP and ALK-1 transcription while keeping CV-2 transcriptional time delay constant at 11 hours. All parameters are used from 3.5.

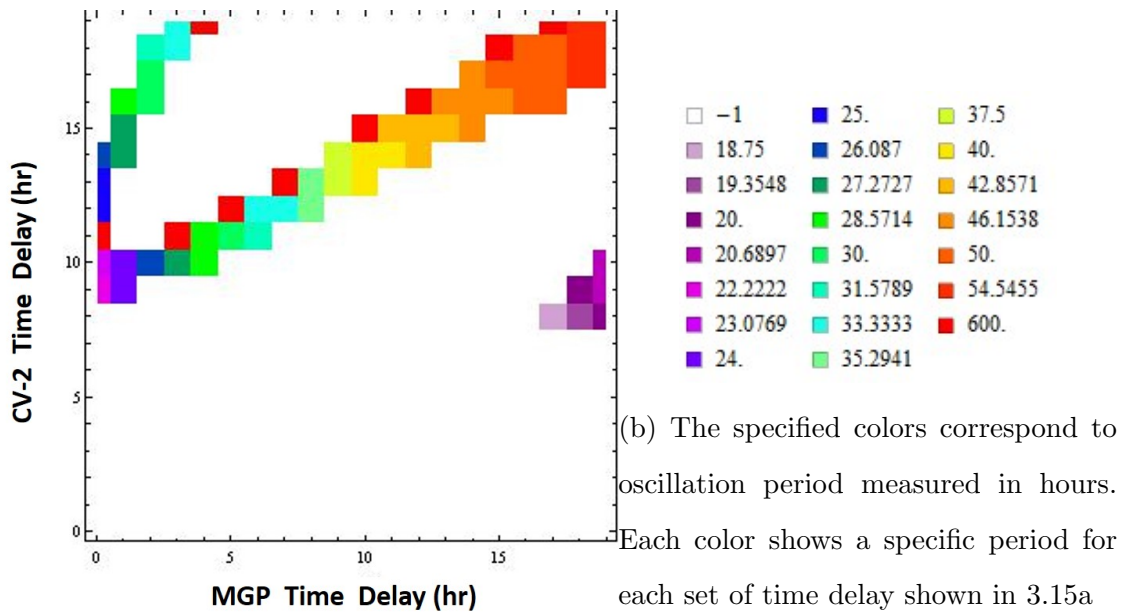


(a) BMP-4



(b) The specified colors correspond to oscillation period measured in hours. Each color shows a specific period for each set of time delay shown in 3.14a

Figure 3.14: **Fourier Analysis of BMP-4:** Oscillation periods are shown with different time delays for CV-2 and ALK-1 transcription while keeping MGP transcriptional time delay constant at 4 hours. All parameters are used from 3.5.



(a) Endoglin

Figure 3.15: **Fourier Analysis of Endoglin:** Oscillation periods are shown with different time delays for MGP and CV-2 transcription while keeping ALK-1 transcriptional time delay constant at 8 hours. All parameters are used from 3.5.

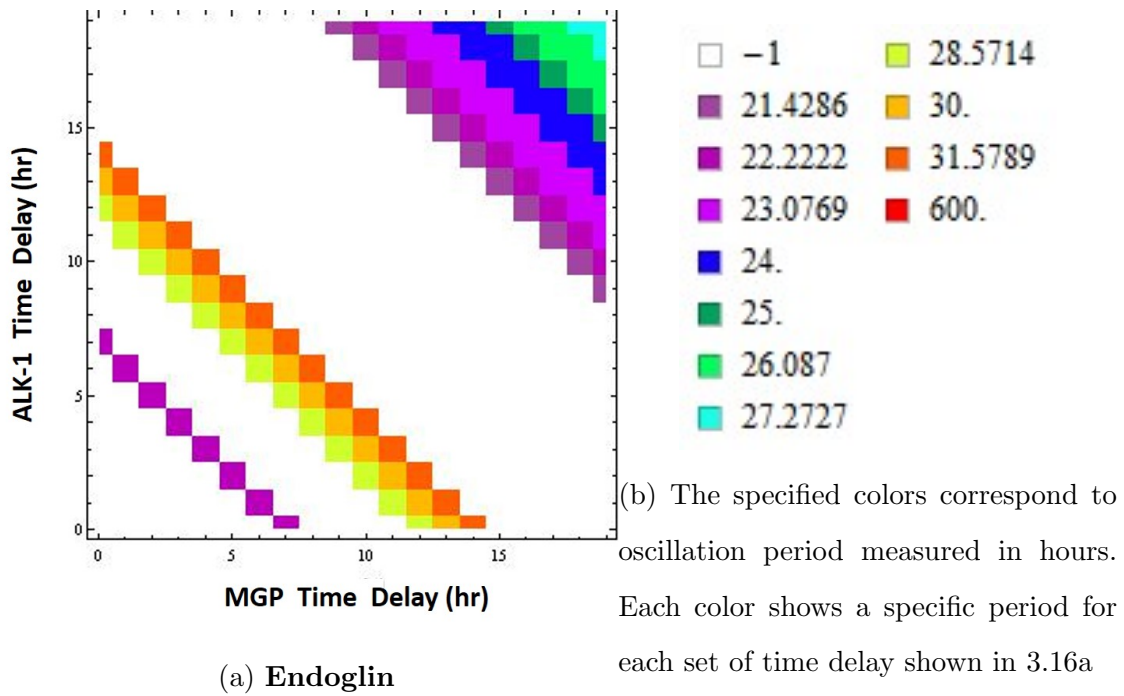
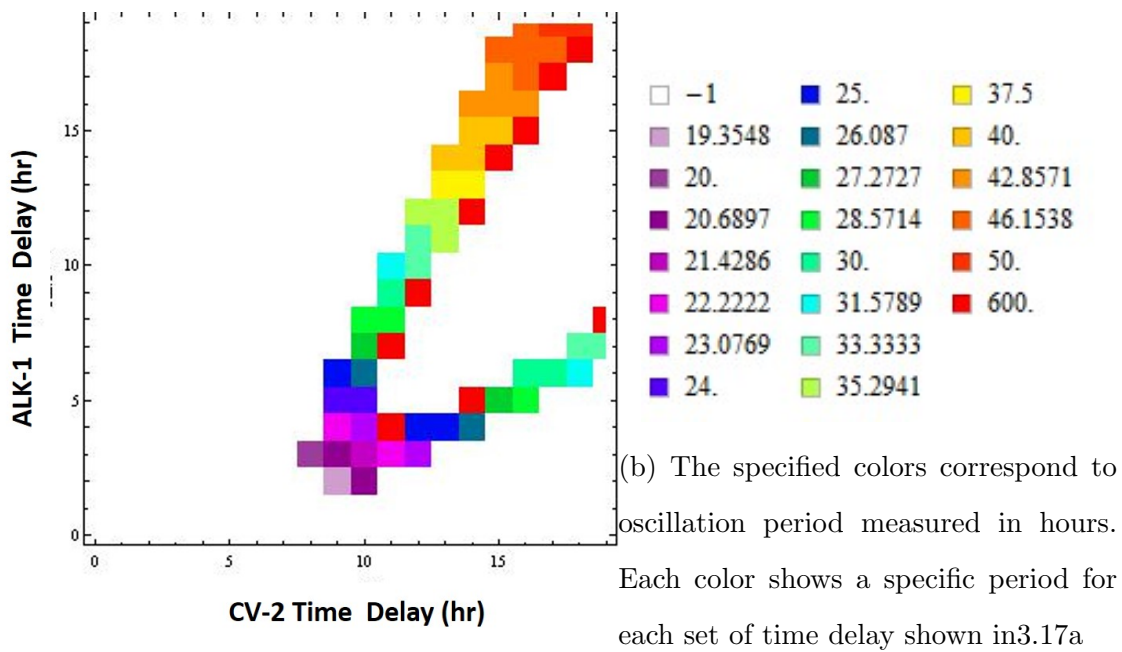
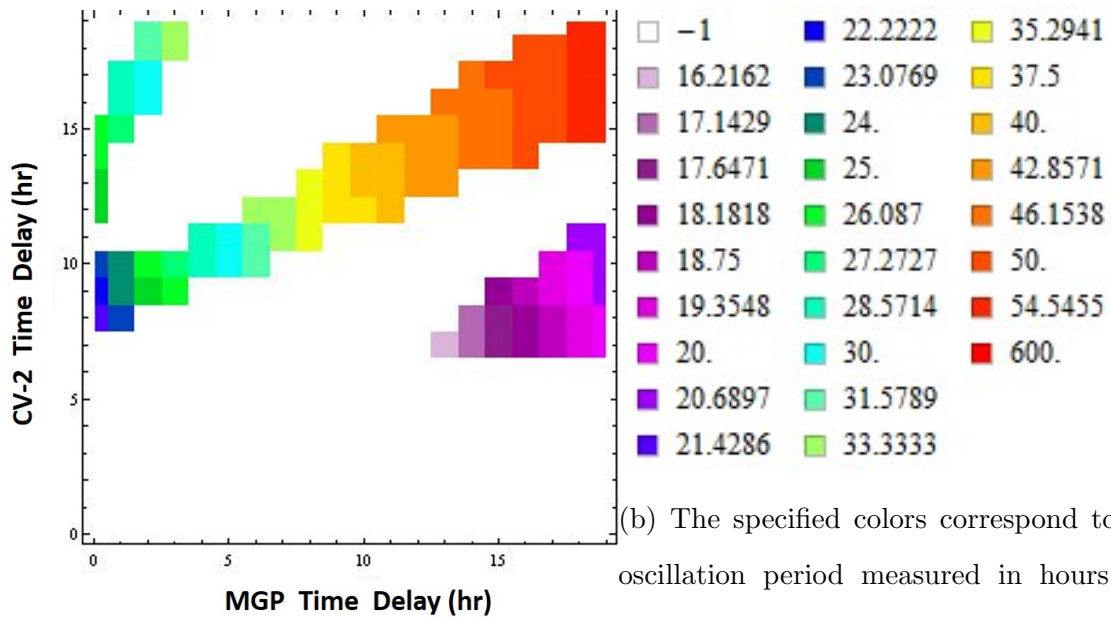


Figure 3.16: **Fourier Analysis of Endoglin:** Oscillation periods are shown with different time delays for MGP and ALK-1 transcription while keeping CV-2 transcriptional time delay constant at 11 hours. All parameters are used from 3.5.



(a) Endoglin

Figure 3.17: **Fourier Analysis of Endoglin:** Oscillation periods are shown with different time delays for CV-2 and ALK-1 transcription while keeping MGP transcriptional time delay constant at 4 hours. All parameters are used from 3.5.



(a) MGP

(b) The specified colors correspond to oscillation period measured in hours. Each color shows a specific period for each set of time delay shown in 3.18a

Figure 3.18: **Fourier Analysis of MGP:** Oscillation periods are shown with different time delays for MGP and CV-2 transcription while keeping ALK-1 transcriptional time delay constant at 8 hours. All parameters are used from 3.5.

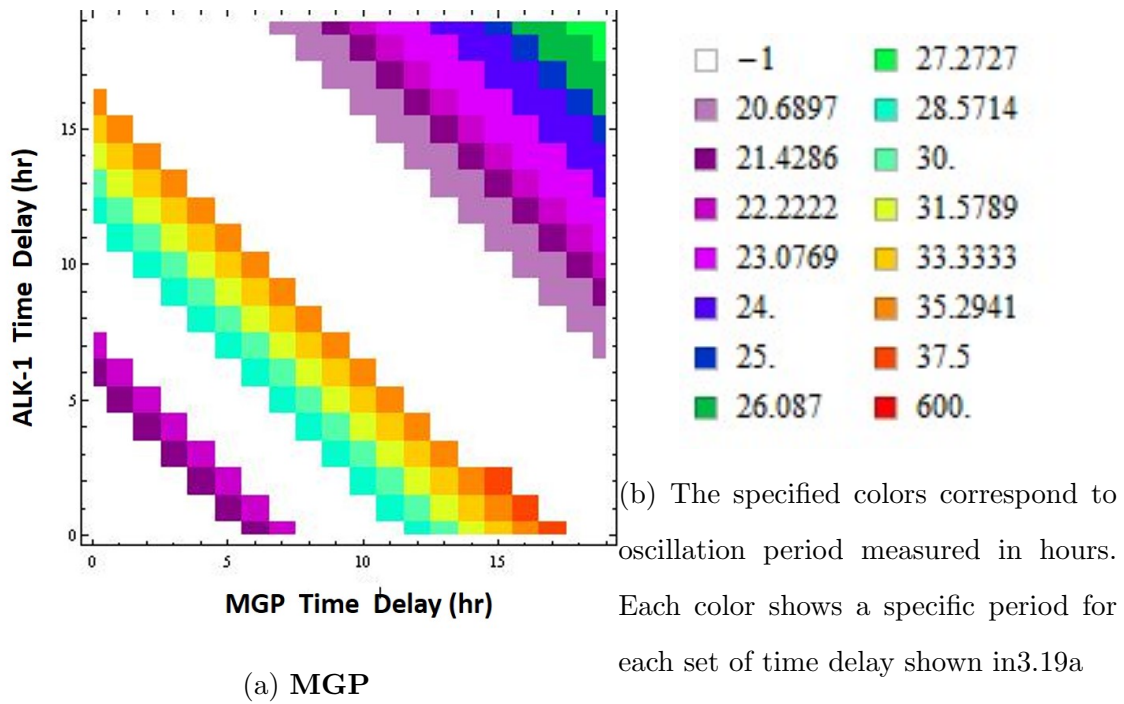


Figure 3.19: **Fourier Analysis of MGP:** Oscillation periods are shown with different time delays for MGP and ALK-1 transcription while keeping CV-2 transcriptional time delay constant at 11 hours. All parameters are used from 3.5.

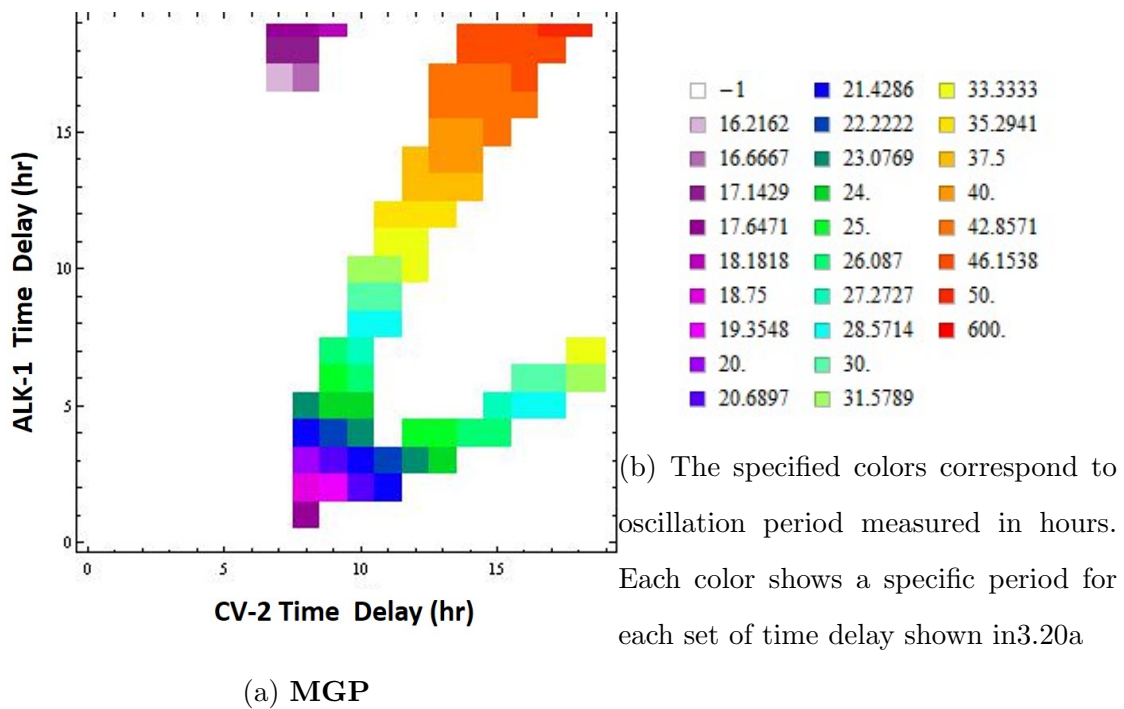
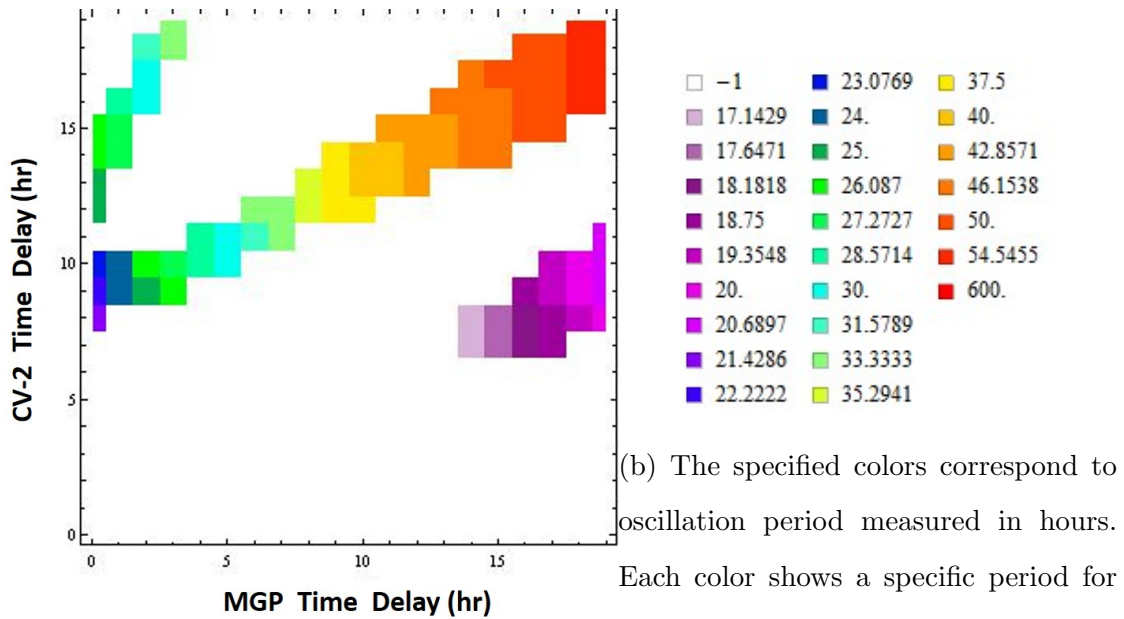
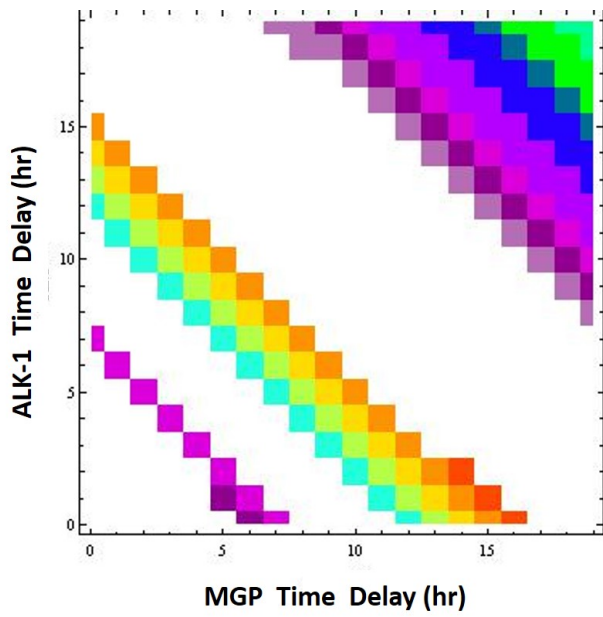


Figure 3.20: **Fourier Analysis of MGP:** Oscillation periods are shown with different time delays for CV-2 and ALK-1 transcription while keeping MGP transcriptional time delay constant at 4 hours. All parameters are used from 3.5

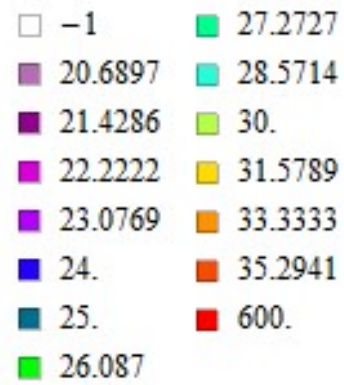


(a) CV-2

Figure 3.21: **Fourier Analysis of CV-2:** Oscillation periods are shown with different time delays for MGP and CV-2 transcription while keeping ALK-1 transcriptional time delay constant at 8 hours. All parameters are used from 3.5.

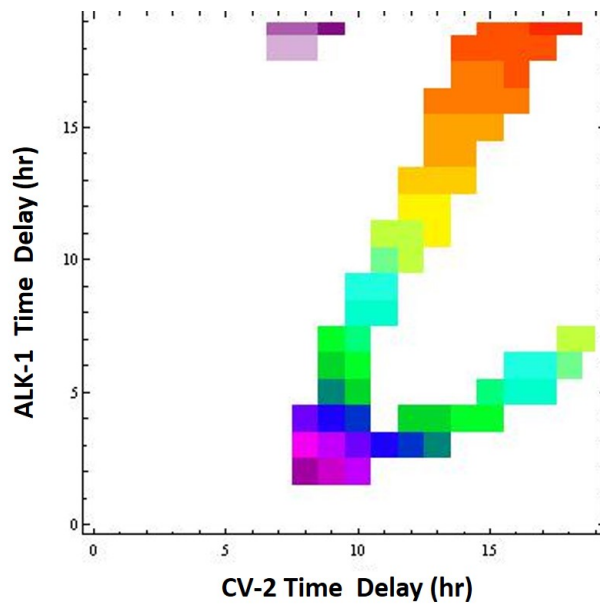


(a) CV-2

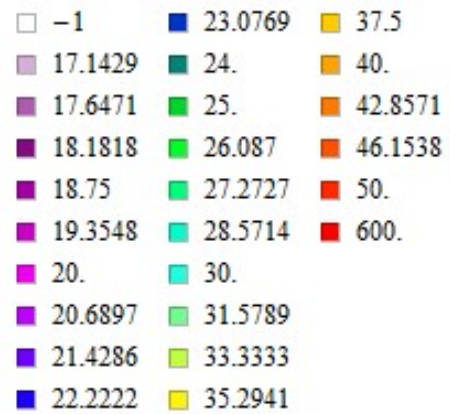


(b) The specified colors correspond to oscillation period measured in hours. Each color shows a specific period for each set of time delay shown in 3.22a

Figure 3.22: **Fourier Analysis of CV-2:** Oscillation periods are shown with different time delays for MGP and ALK-1 transcription while keeping CV-2 transcriptional time delay constant at 11 hours. All parameters are used from 3.5.



(a) CV-2



(b) The specified colors correspond to oscillation period measured in hours. Each color shows a specific period for each set of time delay shown in 3.23a

Figure 3.23: **Fourier Analysis of CV-2:** Oscillation periods are shown with different time delays for CV-2 and ALK-1 transcription while keeping MGP transcriptional time delay constant at 4 hours. All parameters are used from 3.5

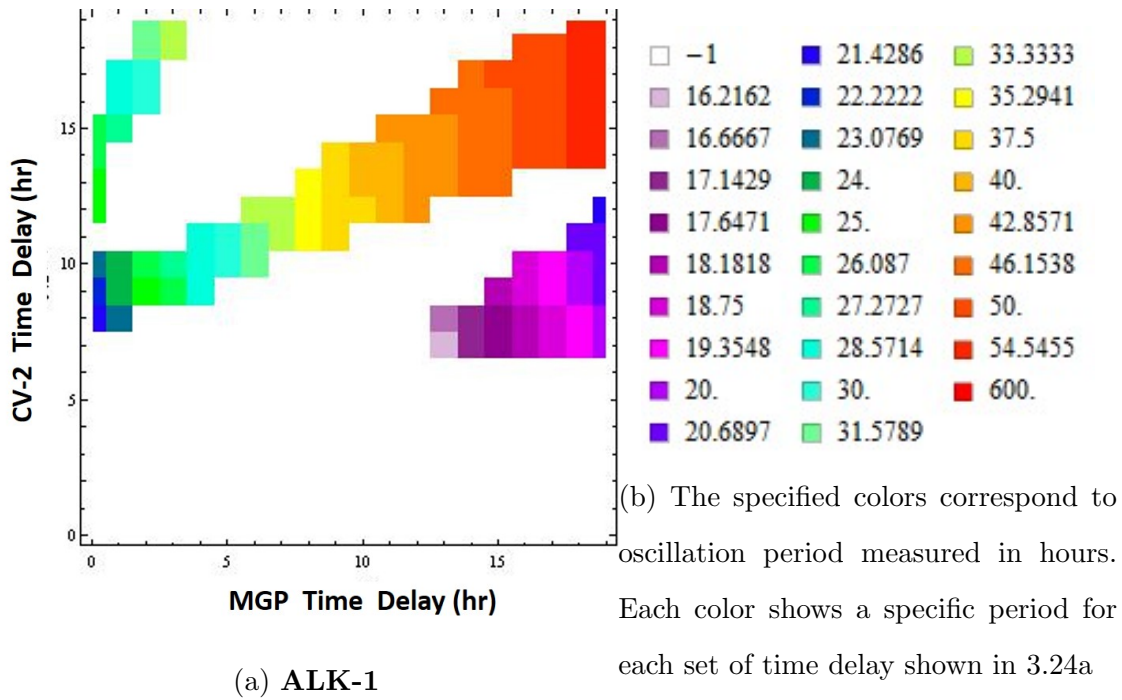


Figure 3.24: **Fourier Analysis of ALK-1:** Oscillation periods are shown with different time delays for MGP and CV-2 transcription while keeping ALK-1 transcriptional time delay constant at 8 hours. All parameters are used from 3.5.

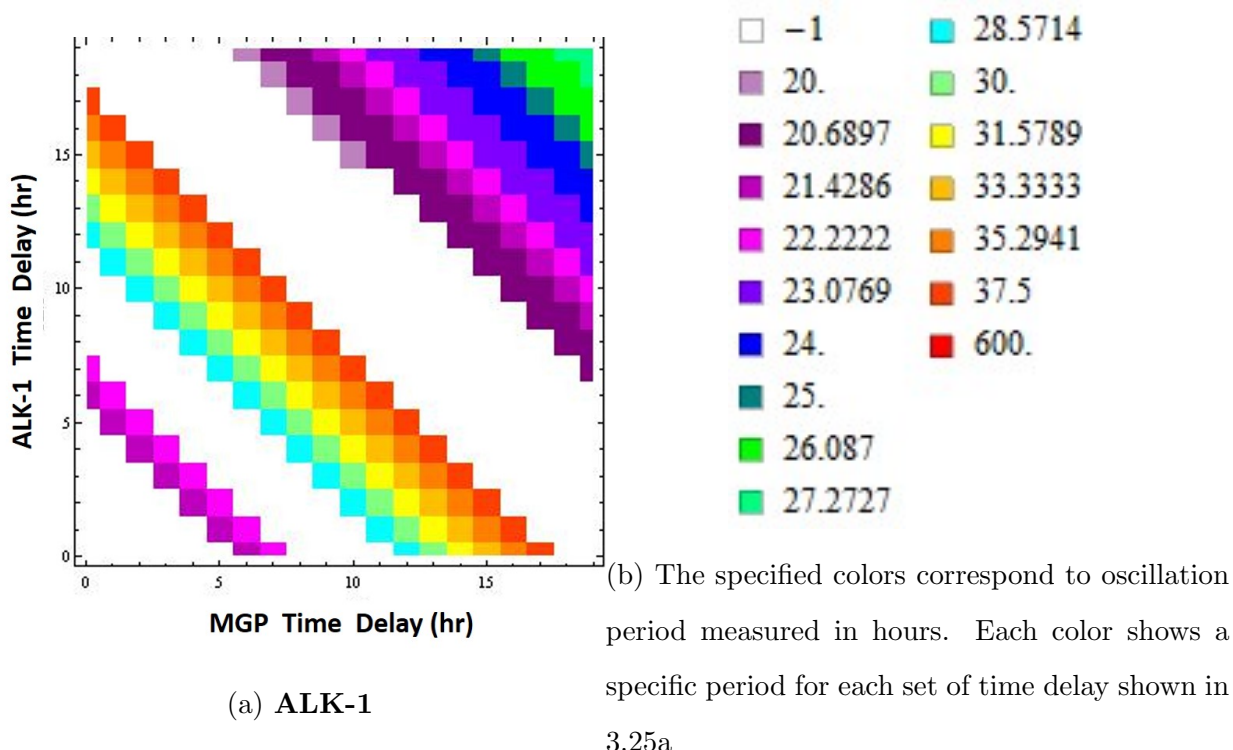


Figure 3.25: **Fourier Analysis of ALK-1:** Oscillation periods are shown with different time delays for MGP and ALK-1 transcription while keeping CV-2 transcriptional time delay constant at 11 hours. All parameters are used from 3.5.

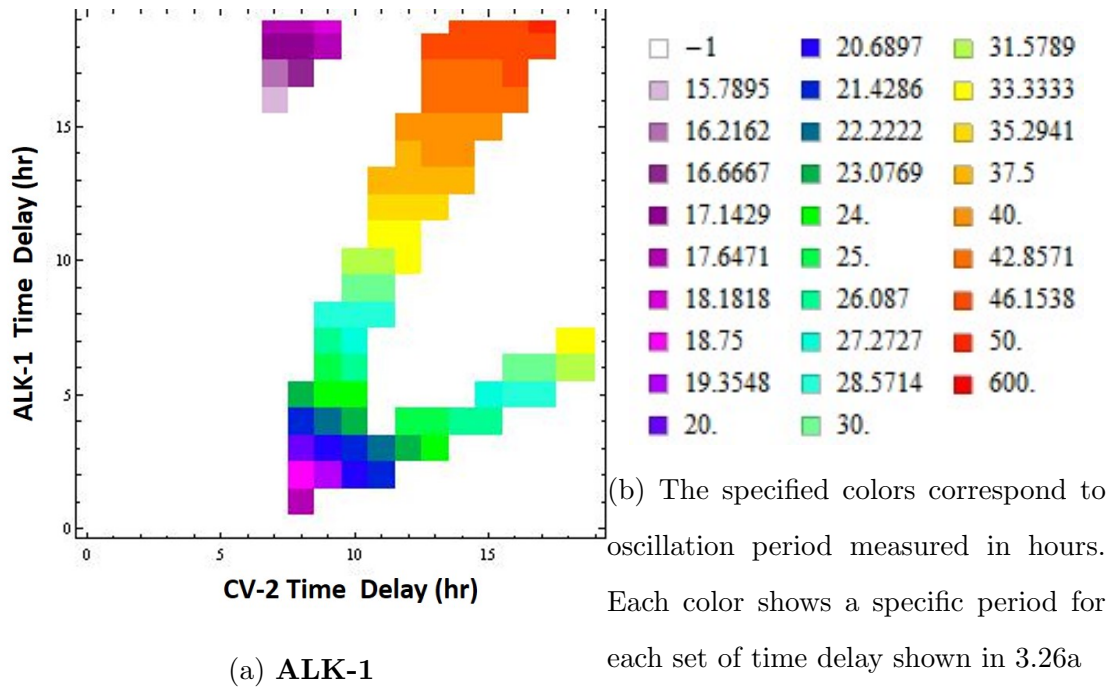


Figure 3.26: **Fourier Analysis of ALK-1:** Oscillation periods are shown with different time delays for CV-2 and ALK-1 transcription while keeping MGP transcriptional time delay constant at 4 hours. All parameters are used from 3.5

CHAPTER 4

Discussion

Oscillations play an important role in many dynamic biological processes. They emerge from the collective interactions of individual entities within the system. Many of the biological oscillations share general features, and theoretical approaches like mathematical modeling are essential for an intuitive understanding of the underlying principles of these biological oscillations.

Negative feedback loops are common in many regulatory networks, particularly in biology, where they regulate transcriptional and post-transcriptional activities. Negative feedback systems usually consist of two genes that mutually control each other. In recent years, mathematical models have been proposed to illustrate the mechanisms of signaling pathways in differentiation. As an example, somite formation is controlled by oscillatory gene expressions that are themselves controlled by the Notch pathway, the Wnt pathway, and the FGF pathway ([5][22][17][56]). These pathways are the main components of the segmentation clock ([5]). The first mathematical model of the Notch pathway was developed by Lewis et al., 2003, in which the researchers modeled the oscillations of Her1/7 gene expression by a single negative feedback loop that is formed by the inhibition of Her1/7 protein ([37]). Later on, a more involved mathematical model was developed by Terry et al., 2011, that had transcriptional time delays ([58][64]).

Currently, there is no study indicating the dynamics of BMP oscillations and their po-

tential role in vascular endothelial cellular differentiation. Our current model investigates the mechanism of oscillatory gene expressions of the BMP system and the cross-talk between BMP-4 and BMP-9 pathways. Here, we characterized a multi-negative feedback loop which are not very well understood in biology. In particular, we explored the dynamics of a feedback system consisting of BMP-9, BMP-4, Endoglin, MGP, CV-2, and ALK-1, which are critical for vascular endothelial differentiation and angiogenesis ([59][12][67][66]). We mathematically modeled this oscillatory regulatory gene expression network and focused on studying the mechanisms for maintaining stable oscillations through a series of simulation experiments. A group of important parameters that can significantly influence oscillations were determined. We have found that stable oscillations can be lost due to disturbing some parameters even in small ranges. From the current analysis of this theoretical model complemented with experimental results of Dr. Bostrom's lab at UCLA, we infer that *degradation rates and time delays are the main causes of maintaining the stable oscillations of this particular BMP-4/9 multi-negative feedback regulatory network.*

In order to capture the oscillatory dynamics that would satisfy the four conditions mentioned in the result section above, we had to increase the degradation rates of Endoglin, MGP, and CV-2 to 80 percent of their production rates and reduced ALK-1 and BMP-9 degradation rates to 65 and 20 percent of their production rates, respectively. We obtain sustained oscillations as shown above in figure 3.5 with periods of oscillations around 24 hours with time delays of 4, 11, and 8 hours, respectively. We identified this set of time delays as our best candidate for several reasons. First, they satisfy the conditions set by the biological experiments. Second, oscillations of 24 hour periods or 1 day has been consistent with most of the experimental results. Last, all time delays are less than 15 hours, which are more physiologically reasonable.

As shown in figure 3.6, all target gene activities are expressed with an oscillatory pattern and their oscillatory period is about 24 hours. In addition, they oscillate synchronously and they are in phase with each other. The results are in good agreement with the results

derived from wet experiments with the exception of BMP-9 and ALK-1, where there are no oscillations in the production of these proteins. However, gene production is different from the activity of these genes. We speculate that the oscillations might indeed occur in the activity levels of BMP-9 and ALK-1 over time as shown in the simulations of figure 3.6. The simulation results along with Fourier analysis results indicate that the high degradation rates of Endoglin, MGP, and CV-2 are required to produce oscillations that would have periods of 24 hours. The mechanisms of proteins degradation are numerous. When biologists talk about degradation, they often refer to proteosomal degradation, a process in which proteins are selected for proteolysis. However, in mathematical models, the degradation terms encompass the larger definition, where it could mean degradation by other processes, such as enzymatic deactivation, binding to extra-cellular matrix, binding to other proteins, endocytosis, and many other routes. As a result, we postulate high degradation rates, as high as 80 percent of Endoglin, MGP, and CV-2 are required in order to achieve oscillatory dynamics of periods of 24 hours, as seen in unpublished experimental results by Dr. Bostrom's lab at UCLA. This would indeed act as a mechanism to regulate progenitor EC differentiation into mature ECs.

Our simulation experiments with degradation rates in order to produce stable oscillations have revealed that *low degradation rate of BMP-4 is critical for oscillations. In addition, high degradation rates of Endoglin, MGP, and CV-2 are also critical in order to produce stable oscillations.* MGP is an inhibitor of BMP-4 and its high degradation rate would be in line with higher levels of BMP-4. Furthermore, using lower time delays in order to produce 24 hour period oscillations requires the ALK-1 degradation rate to be lower than the rest of the variables. Since ALK-1 is produced by BMP-4, higher levels of BMP-4 would also require higher levels of ALK-1. The presence of BMP-4 and ALK-1 induced oscillations, while too much Endoglin, MGP, and CV-2 would quench oscillations. We speculate that different degradation rates in different tissues could be key to different control of oscillatory regime behavior.

4.1 Time Delay Analysis using the Fourier Transform Method

Time delays are often not considered in differential equations, since they add tremendous complexity to analyzing the model. However, in our current model, time delays are essential for the production of oscillations and have been observed in biological experimental results as well. We performed Fourier analysis to recognize the important time delay parameters to identify the stable oscillations of the system that would satisfy the conditions mentioned above. One of the conditions that had to be satisfied was that the time delay of the CV-2 expression in vascular endothelial cells had to be greater than the time delay of MGP expression, and the difference between the two was about 7-8 hours. In addition, we are only interested in finding those oscillations that are about 24 hours long. The Fourier analysis of each individual time delay set for individual variables revealed that there are only certain regions where these conditions are met. In particular, time delay set of 4, 11, and 8 hours has been identified as the best candidate for the system's time delays.

4.2 Conclusion

In this study, we proposed a mathematical model to simulate the dynamics of the BMP-9/4 pathways in ECs and focused on studying the mechanisms for maintaining stable oscillations through a series of simulation experiments and Fourier analysis. The simulation results show that it is feasible to obtain stable oscillations that meet our conditions, if we increase the degradation rates of Endoglin, CV-2, and MGP while keeping more BMP-4 in the system. A group of important parameters that can significantly affect the oscillations are degradation rates and the time delays. In addition, we have found that when oscillation is lost due to changing the time delays, it can be rescued by changing the degradation rates. In other words, stable oscillations can be rescued when the degradation rates of Endoglin, CV-2, and MGP are 60 percent of their production rates with longer time delays. However, the

drawback of that would be that the period of oscillations are unusually larger than our expected 24 hour outcome. Achieving 24 hour periodic oscillations would require increasing those degradation rates. In addition, we inferred that multi-negative feedback loops are one of the main regulators of stable oscillations in BMP gene expression.

REFERENCES

- [1] CureHHT.
- [2] Morten Andersen, Frank Vinther, and Johnny T. Ottesen. Mathematical modeling of the hypothalamic-pituitary-adrenal gland (HPA) axis, including hippocampal mechanisms. *Mathematical Biosciences*, 246(1):122–138, November 2013.
- [3] Gregory J. Anderson, Deepak Darshan, Sarah J. Wilkins, and David M. Frazer. Regulation of systemic iron homeostasis: how the body responds to changes in iron demand. *Biometals*, 20(3-4):665–674, February 2007.
- [4] Richard C. Aster, Brian Borchers, and Clifford H. Thurber. *Parameter Estimation and Inverse Problems*. Academic Press, December 2011.
- [5] Alexander Aulehla and Olivier Pourqui. Oscillating signaling pathways during embryonic development. *Current Opinion in Cell Biology*, 20(6):632–637, December 2008.
- [6] Hao Bai, Yongxing Gao, Melanie Arzigian, Don M. Wojchowski, Wen-shu Wu, and Zack Z. Wang. BMP4 regulates vascular progenitor development in human embryonic stem cells through a smad-dependent pathway. *J. Cell. Biochem.*, 109(2):363–374, February 2010.
- [7] Y. Bard. Comparison of Gradient Methods for the Solution of Nonlinear Parameter Estimation Problems. *SIAM J. Numer. Anal.*, 7(1):157–186, March 1970.
- [8] James Vere Beck and Kenneth J. Arnold. *Parameter Estimation in Engineering and Science*. James Beck, 1977.
- [9] A. Becskei. Positive feedback in eukaryotic gene networks: cell differentiation by graded to binary response conversion. *The EMBO Journal*, 20(10):2528–2535, May 2001.
- [10] Francisco J. Blanco, Juan F. Santibanez, Mercedes Guerrero-Esteo, Carmen Langa, Calvin P.H. Vary, and Carmelo Bernabeu. Interaction and functional interplay between endoglin and ALK-1, two components of the endothelial transforming growth factor-receptor complex. *J. Cell. Physiol.*, 204(2):574–584, August 2005.
- [11] L. M. Botella, T. Snchez-Elsner, C. Rius, A. Corb, and C. Bernabu. Identification of a critical Sp1 site within the endoglin promoter and its involvement in the transforming growth factor-beta stimulation. *J. Biol. Chem.*, 276(37):34486–34494, September 2001.
- [12] N. L. Boyd, S. K. Dhara, R. Rekaya, E. A. Godbey, K. Hasneen, R. R. Rao, F. D. West, B. A. Gerwe, and S. L. Stice. BMP4 Promotes Formation of Primitive Vascular Networks in Human Embryonic Stem Cell-Derived Embryoid Bodies. *Exp Biol Med (Maywood)*, 232(6):833–843, June 2007.

- [13] Monica A. Brown, Qinghai Zhao, Kent A. Baker, Chethana Naik, Cecil Chen, Laurie Pukac, Mallika Singh, Tatiana Tsareva, Yanick Parice, Angela Mahoney, Viktor Roschke, Indra Sanyal, and Senyon Choe. Crystal Structure of BMP-9 and Functional Interactions with Pro-region and Receptors. *J. Biol. Chem.*, 280(26):25111–25118, July 2005.
- [14] Cecil Chen, Krzysztof J. Grzegorzewski, Steve Barash, Qinghai Zhao, Helmut Schneider, Qi Wang, Mallika Singh, Laurie Pukac, Adam C. Bell, Roxanne Duan, Tim Coleman, Alokesh Duttaroy, Susan Cheng, Jon Hirsch, Linyi Zhang, Yanick Lazard, Carrie Fischer, Melisa Carey Barber, Zhi-Dong Ma, Ya-Qin Zhang, Peter Reavey, Lilin Zhong, Baiqin Teng, Indra Sanyal, Steve M. Ruben, Olivier Blondel, and Charles E. Birse. An integrated functional genomics screening program reveals a role for BMP-9 in glucose homeostasis. *Nat Biotech*, 21(3):294–301, March 2003.
- [15] Ting-Hsuan Chen, Chunyan Guo, Xin Zhao, Yucheng Yao, Kristina I. Boström, Margaret N. Wong, Yin Tintut, Linda L. Demer, Chih-Ming Ho, and Alan Garfinkel. Patterns of periodic holes created by increased cell motility. *Interface Focus*, page rfs20120001, March 2012.
- [16] I-Chun Chou and Eberhard O. Voit. Recent developments in parameter estimation and structure identification of biochemical and genomic systems. *Mathematical Biosciences*, 219(2):57–83, June 2009.
- [17] J. Cooke. A gene that resuscitates a theory—somitogenesis and a molecular oscillator. *Trends Genet.*, 14(3):85–88, March 1998.
- [18] J. Cooke and E. C. Zeeman. A clock and wavefront model for control of the number of repeated structures during animal morphogenesis. *Journal of Theoretical Biology*, 58(2):455–476, 1976.
- [19] Tal Danino, Dmitri Volfson, Sangeeta N. Bhatia, Lev Tsimring, and Jeff Hasty. In-Silico Patterning of Vascular Mesenchymal Cells in Three Dimensions. *PLoS ONE*, 6(5):e20182, May 2011.
- [20] Laurent David, Christine Mallet, Michelle Keramidas, Nol Lamand, Jean-Marie Gasc, Sophie Dupuis-Girod, Henri Plauchu, Jean-Jacques Feige, and Sabine Bailly. Bone Morphogenetic Protein-9 Is a Circulating Vascular Quiescence Factor. *Circulation Research*, 102(8):914–922, April 2008.
- [21] E. Ronald de Kloet, Erno Vreugdenhil, Melly S. Oitzl, and Marian Jols. Brain Corticosteroid Receptor Balance in Health and Disease. *Endocrine Reviews*, 19(3):269–301, June 1998.
- [22] Mary-Lee Dequant and Olivier Pourqui. Segmental patterning of the vertebrate embryonic axis. *Nat Rev Genet*, 9(5):370–382, May 2008.
- [23] P. ten Dijke, H. Yamashita, H. Ichijo, P. Franzen, M. Laiho, K. Miyazono, and C. H. Heldin. Characterization of type I receptors for transforming growth factor-beta and activin. *Science*, 264(5155):101–104, April 1994.

- [24] E. V. Entchev, A. Schwabedissen, and M. Gonzalez-Gaitn. Gradient formation of the TGF-beta homolog Dpp. *Cell*, 103(6):981–991, December 2000.
- [25] Irving R. Epstein and Kenneth Showalter. Nonlinear Chemical Dynamics: Oscillations, Patterns, and Chaos. *J. Phys. Chem.*, 100(31):13132–13147, January 1996.
- [26] Francisco Jos Fernandez-Fernandez. Hereditary haemorrhagic telangiectasia: From symptomatic management to pathogenesis based treatment. *Eur J Hum Genet*, 18(4):404, April 2010.
- [27] W. O. Friesen and G. D. Block. What is a biological oscillator? *American Journal of Physiology - Regulatory, Integrative and Comparative Physiology*, 246(6):R847–R853, June 1984.
- [28] Alan Garfinkel, Yin Tintut, Danny Petrusek, Kristina Boström, and Linda L. Demer. Pattern formation by vascular mesenchymal cells. *PNAS*, 101(25):9247–9250, June 2004.
- [29] Marie-Jos Goumans, Gudrun Valdimarsdottir, Susumu Itoh, Alexander Rosendahl, Paschalis Sideras, and Peter ten Dijke. Balancing the activation state of the endothelium via two distinct TGF- typeI receptors. *EMBO J*, 21(7):1743–1753, April 2002.
- [30] Brigid LM Hogan. Bone morphogenetic proteins in development. *Current Opinion in Genetics & Development*, 6(4):432–438, August 1996.
- [31] Frank Jlicher and Jacques Prost. Spontaneous Oscillations of Collective Molecular Motors. *Phys. Rev. Lett.*, 78(23):4510–4513, June 1997.
- [32] D. W. Johnson, J. N. Berg, M. A. Baldwin, C. J. Gallione, I. Marondel, S.-J. Yoon, T. T. Stenzel, M. Speer, M. A. Pericak-Vance, A. Diamond, A. E. Gutmacher, C. E. Jackson, L. Attisano, R. Kucherlapati, M. E. M. Porteous, and D. A. Marchuk. Mutations in the activin receptorlike kinase 1 gene in hereditary haemorrhagic telangiectasia type 2. *Nat Genet*, 13(2):189–195, June 1996.
- [33] Q. Kang, M. H. Sun, H. Cheng, Y. Peng, A. G. Montag, A. T. Deyrup, W. Jiang, H. H. Luu, J. Luo, J. P. Szatkowski, P. Vanichakarn, J. Y. Park, Y. Li, R. C. Haydon, and T.-C. He. Characterization of the distinct orthotopic bone-forming activity of 14 BMPs using recombinant adenovirus-mediated gene delivery. *Gene Ther*, 11(17):1312–1320, July 2004.
- [34] Karsten Kruse and Frank Jlicher. Oscillations in cell biology. *Current Opinion in Cell Biology*, 17(1):20–26, February 2005.
- [35] P. Lastres, A. Letamenda, H. Zhang, C. Rius, N. Almendro, U. Raab, L. A. Lopez, C. Langa, A. Fabra, M. Letarte, and C. Bernabu. Endoglin modulates cellular responses to TGF-beta 1. *J Cell Biol*, 133(5):1109–1121, June 1996.
- [36] Franck Lebrin, Marie-Jos Goumans, Leon Jonker, Rita L C Carvalho, Gudrun Valdimarsdottir, Midory Thorikay, Christine Mummery, Helen M Arthur, and Peter ten Dijke. Endoglin promotes endothelial cell proliferation and TGF-/ALK1 signal transduction. *The EMBO Journal*, 23(20):4018–4028, October 2004.

- [37] Julian Lewis. Autoinhibition with Transcriptional Delay: A Simple Mechanism for the Zebrafish Somitogenesis Oscillator. *Current Biology*, 13(16):1398–1408, August 2003.
- [38] Dean Y. Li, Lise K. Sorensen, Benjamin S. Brooke, Lisa D. Urness, Elaine C. Davis, Douglas G. Taylor, Beth B. Boak, and Daniel P. Wendel. Defective Angiogenesis in Mice Lacking Endoglin. *Science*, 284(5419):1534–1537, May 1999.
- [39] K. A. McAllister, K. M. Grogg, D. W. Johnson, C. J. Gallione, M. A. Baldwin, C. E. Jackson, E. A. Helmbold, D. S. Markel, W. C. McKinnon, J. Murrel, M. K. McCormick, M. A. Pericak-Vance, P. Heutink, B. A. Oostra, T. Haitjema, C. J. J. Westerman, M. E. Porteous, A. E. Guttmacher, M. Letarte, and D. A. Marchuk. Endoglin, a TGF- binding protein of endothelial cells, is the gene for hereditary haemorrhagic telangiectasia type 1. *Nat Genet*, 8(4):345–351, December 1994.
- [40] Aaron F. Miller, Stephen A. K. Harvey, R. Scott Thies, and Merle S. Olson. Bone Morphogenetic Protein-9 AN AUTOCRINE/PARACRINE CYTOKINE IN THE LIVER. *J. Biol. Chem.*, 275(24):17937–17945, June 2000.
- [41] Nicholas A. M. Monk. Oscillatory Expression of Hes1, p53, and NF-B Driven by Transcriptional Time Delays. *Current Biology*, 13(16):1409–1413, August 2003.
- [42] W. Oelkers. Clinical diagnosis of hyper- and hypocortisolism. *Noise Health*, 2(7):39–48, 2000.
- [43] S. Paul Oh, Tsugio Seki, Kendrick A. Goss, Takeshi Imamura, Youngsuk Yi, Patricia K. Donahoe, Li Li, Kohei Miyazono, Peter ten Dijke, Seongjin Kim, and En Li. Activin receptor-like kinase 1 modulates transforming growth factor-1 signaling in the regulation of angiogenesis. *PNAS*, 97(6):2626–2631, March 2000.
- [44] R. W. Padgett, J. M. Wozney, and W. M. Gelbart. Human BMP sequences can confer normal dorsal-ventral patterning in the Drosophila embryo. *PNAS*, 90(7):2905–2909, April 1993.
- [45] M. P. Panchenko, M. C. Williams, J. S. Brody, and Q. Yu. Type I receptor serine-threonine kinase preferentially expressed in pulmonary blood vessels. *Am. J. Physiol.*, 270(4 Pt 1):L547–558, April 1996.
- [46] Sybill Patan. Vasculogenesis and angiogenesis. *Cancer Treat. Res.*, 117:3–32, 2004.
- [47] A. Peters, U. Schweiger, L. Pellerin, C. Hubold, K. M. Oltmanns, M. Conrad, B. Schultes, J. Born, and H. L. Fehm. The selfish brain: competition for energy resources. *Neurosci Biobehav Rev*, 28(2):143–180, April 2004.
- [48] W. Risau, P. Gautschi-Sova, and P. Bhlen. Endothelial cell growth factors in embryonic and adult chick brain are related to human acidic fibroblast growth factor. *EMBO J.*, 7(4):959–962, April 1988.
- [49] Bernard A.J. Roelen, Marga A. van Rooijen, and Christine L. Mummery. Expression of ALK-1, a type 1 serine/threonine kinase receptor, coincides with sites of vasculogenesis and angiogenesis in early mouse development. *Dev. Dyn.*, 209(4):418–430, August 1997.

- [50] C. Rus, J. D. Smith, N. Almendro, C. Langa, L. M. Botella, D. A. Marchuk, C. P. Vary, and C. Bernabu. Cloning of the promoter region of human endoglin, the target gene for hereditary hemorrhagic telangiectasia type 1. *Blood*, 92(12):4677–4690, December 1998.
- [51] Marion Scharpfenecker, M. van Dinther, Zhen Liu, R. L. van Bezooijen, Qinghai Zhao, Laurie Pukac, Clemens W. G. M. Lwik, and P. ten Dijke. BMP-9 signals via ALK1 and inhibits bFGF-induced endothelial cell proliferation and VEGF-stimulated angiogenesis. *J Cell Sci*, 120(6):964–972, March 2007.
- [52] Annette Schuler-Metz, Sigrun Knchel, Eckhard Kaufmann, and Walter Knchel. The Homeodomain Transcription Factor Xvent-2 Mediates Autocatalytic Regulation of BMP-4 Expression in Xenopus Embryos. *J. Biol. Chem.*, 275(44):34365–34374, November 2000.
- [53] Tsugio Seki, Jihye Yun, and S. Paul Oh. Arterial Endothelium-Specific Activin Receptor-Like Kinase 1 Expression Suggests Its Role in Arterialization and Vascular Remodeling. *Circulation Research*, 93(7):682–689, October 2003.
- [54] Esther S. Shao, Laura Lin, Yucheng Yao, and Kristina I. Bostrm. Expression of vascular endothelial growth factor is coordinately regulated by the activin-like kinase receptors 1 and 5 in endothelial cells. *Blood*, 114(10):2197–2206, September 2009.
- [55] Tilman Snchez-Elsner, Luisa M. Botella, Beatriz Velasco, Carmen Langa, and Carmelo Bernabu. Endoglin Expression Is Regulated by Transcriptional Cooperation between the Hypoxia and Transforming Growth Factor- Pathways. *J. Biol. Chem.*, 277(46):43799–43808, November 2002.
- [56] Heather L. Stickney, Michael J.F. Barresi, and Stephen H. Devoto. Somite development in zebrafish. *Dev. Dyn.*, 219(3):287–303, November 2000.
- [57] Steven H. Strogatz. *Nonlinear Dynamics and Chaos: With Applications to Physics, Biology, Chemistry, and Engineering*. Westview Press, August 2014.
- [58] Alan J. Terry, Marc Sturrock, J. Kim Dale, Miguel Maroto, and Mark A. J. Chaplain. A Spatio-Temporal Model of Notch Signalling in the Zebrafish Segmentation Clock: Conditions for Synchronised Oscillatory Dynamics. *PLoS ONE*, 6(2):e16980, February 2011.
- [59] Valentine Thorimbert, Dsire Knig, Jan Marro, Florence Ruggiero, and Anna Jawiska. Bone morphogenetic protein signaling promotes morphogenesis of blood vessels, wound epidermis, and actinotrichia during fin regeneration in zebrafish. *FASEB J.*, July 2015.
- [60] David Umulis, Michael B. O’Connor, and Seth S. Blair. The extracellular regulation of bone morphogenetic protein signaling. *Development*, 136(22):3715–3728, November 2009.
- [61] Marshall R. Urist. Bone: Formation by Autoinduction. *Science*, 150(3698):893–899, November 1965.

- [62] Lisa D. Urness, Lise K. Sorensen, and Dean Y. Li. Arteriovenous malformations in mice lacking activin receptor-like kinase-1. *Nat Genet*, 26(3):328–331, November 2000.
- [63] Frank Vinther, Morten Andersen, and Johnny T. Ottesen. The minimal model of the hypothalamicpituitaryadrenal axis. *J. Math. Biol.*, 63(4):663–690, November 2010.
- [64] Hong-yan Wang, Yan-xin Huang, Li-hua Zheng, Yong-li Bao, Lu-guo Sun, Yin Wu, Chun-lei Yu, Zhen-bo Song, Ying Sun, Guan-nan Wang, Zhi-qiang Ma, and Yu-xin Li. Modelling coupled oscillations in the Notch, Wnt, and FGF signaling pathways during somitogenesis: a comprehensive mathematical model. *Comput Intell Neurosci*, 2015:387409, 2015.
- [65] J. M. Wozney, V. Rosen, A. J. Celeste, L. M. Mitsock, M. J. Whitters, R. W. Kriz, R. M. Hewick, and E. A. Wang. Novel regulators of bone formation: molecular clones and activities. *Science*, 242(4885):1528–1534, December 1988.
- [66] G. D. Yancopoulos, M. Klagsbrun, and J. Folkman. Vasculogenesis, angiogenesis, and growth factors: ephrins enter the fray at the border. *Cell*, 93(5):661–664, May 1998.
- [67] Yucheng Yao, Medet Jumabay, Albert Ly, Melina Radparvar, Anthony H. Wang, Raushan Abdmaulen, and Kristina I. Boström. Crossveinless 2 regulates bone morphogenetic protein 9 in human and mouse vascular endothelium. *Blood*, 119(21):5037–5047, May 2012.
- [68] Yucheng Yao, Medet Jumabay, Anthony Wang, and Kristina I. Boström. Matrix Gla protein deficiency causes arteriovenous malformations in mice. *J Clin Invest*, 121(8):2993–3004, August 2011.
- [69] Daniel Yazdi. Nonlinear time-delay dynamical model of oscillatory gene expression in BMP-4/9 vascular endothelial cell network. *eScholarship*, January 2014.
- [70] Amina F. Zebboudj, Minori Imura, and Kristina Boström. Matrix GLA Protein, a Regulatory Protein for Bone Morphogenetic Protein-2. *J. Biol. Chem.*, 277(6):4388–4394, February 2002.